Petrology and Stratigraphy of the Fra Mauro Formation at the Apollo 14 Site

GEOLOGICAL SURVEY PROFESSIONAL PAPER 785

Prepared on behalf of the
National Aeronautics and Space Administration

Petrology and Stratigraphy of the Fra Mauro Formation at the Apollo 14 Site

By H. G. WILSHIRE *and* E. D. JACKSON

GEOLOGICAL SURVEY PROFESSIONAL PAPER 785

Prepared on behalf of the National Aeronautics and Space Administration

Distribution of Apollo 14 fragmental rocks, classified into four groups, suggests that the Fra Mauro Formation consists of stratified ejecta

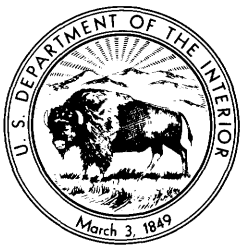

UNITED STATES GOVERNMENT PRINTING OFFICE, WASHINGTON : 1972

UNITED STATES DEPARTMENT OF THE INTERIOR

ROGERS C. B. MORTON, *Secretary*

GEOLOGICAL SURVEY

V. E. McKelvey, *Director*

Library of Congress catalog-card No. 72-600103

For sale by the Superintendent of Documents, U.S. Government Printing Office
Washington, D.C. 20402

CONTENTS

ILLUSTRATIONS

TABLES

PETROLOGY AND STRATIGRAPHY OF THE FRA MAURO FORMATION AT THE APOLLO 14 SITE

By H. G. WILSHIRE and E. D. JACKSON

ABSTRACT

The Apollo 14 rocks returned to earth are divisible into two broad groups: relatively homogeneous crystalline rocks and fragmental rocks (breccias). The crystalline rocks are, for the most part, metaclastic, but a few, including the second largest sample returned, are aphyric basalts. All of the crystalline rocks are considered to be clasts dislodged from fragmental rocks. These fragmental rocks constitute the Fra Mauro Formation, which is presumed to be the ejecta deposit from the Imbrium basin. Megascopic properties of the fragmental rocks suggest a fourfold subdivision: F_1, poorly consolidated breccias with light clasts dominant over dark ones, with few clasts larger than 1 mm, and with comparatively abundant fragmental glass; F_2, coherent breccias with light clasts dominant and with comparatively abundant fragmental glass; F_3, moderately coherent breccias with dark clasts dominant and with no fragmental glass; and F_4, coherent breccias with dark clasts dominant and with no fragmental glass.

Systematic microscopic descriptions and clast counts of 19 different breccias revealed that (1) clasts of fine-grained thermally metamorphosed fragmental rock are by far the dominant type in the breccias; (2) there are eight main varieties of igneous clasts including basalt, anorthosite-gabbro, plagioclase cumulates, and quartz-alkali feldspar intergrowths; (3) a significantly high proportion of mineral clasts occurs in the size range 0.1–1.0 mm; plagioclase is dominant among the mineral clasts, but the proportion of pyroxene is as much as 50 percent; and (4) lithic and mineral clasts commonly are cataclastically deformed.

Most of the rocks contain compound clasts that are themselves pieces of breccia. Two generations of breccia are common, and as many as four occur in the samples studied. The rock types in compound clasts reveal earlier fragmentation-metamorphic episodes that predate the Fra Mauro Formation.

Partial to complete reequilibration reactions have taken place between matrices and clasts in a number of the fragmental rocks. These relations suggest postconsolidation thermal effects on the Fra Mauro Formation. Similar reactions are observed within clasts in all types of fragmental rocks, whether glassy or crystalline. It appears that more than one generation of reequilibration reactions is represented in the Fra Mauro and that older breccias had thermal histories similar to that of the Fra Mauro Formation itself.

The distribution of rocks at the Apollo 14 site suggests that the Fra Mauro Formation is stratified; units of dark-clast-dominant breccias (F_3, F_4) are deepest, and units of light-clast-dominant breccias (F_2) are shallowest. Poorly consolidated glass-rich rocks (F_1) are considered to be weakly lithified regolith, derived either from disaggregated F_1 type breccias or from originally unconsolidated material at the top of the Fra Mauro Formation. This stratigraphic sequence is consistent with the comparative abundance of glass and the weakly developed reequilibration reactions in F_2 rocks and with the dominance of light-colored metaclastic rocks among the lithic fragments of the soils. It is presumed that thermal blanketing of the lower dark-clast-dominant breccias allowed time for reactions to proceed and for annealing and devitrification of glass. Thus, although we see that the Fra Mauro Formation is composed of three or four distinct units based on clast populations, its internal thermal metamorphism appears to be gradational.

The compound clasts and great variety of lithic fragments indicate that the pre-Imbrium terrane, presumed to have existed prior to about 3.9–4.2 billion years ago, was already exceedingly complex. However, the similarity of older breccias to the Fra Mauro breccias themselves indicates that processes such as extrusion of basalt, intrusion and differentiation of basaltic magma, impact brecciation, and metamorphism prior to the Imbrium event were not unlike later events. The complex clasts of the Fra Mauro breccias therefore reveal a long history of impact-related events that probably record half a billion years of planetary accretion, of which the Imbrium impact was one of the last large events.

INTRODUCTION

Apollo 14 landed on an area of lunar terra composed of materials that premission studies indicated were ejecta from the Imbrium basin (Gilbert, 1893; Swann and others, 1971; Swann and Field Geology Team, 1971). This deposit, forming a broad belt surrounding Mare Imbrium, has been designated the Fra Mauro Formation (Eggleton, 1963; Wilhelms, 1970). The landing site (fig. 1) is about 550 km (kilometers) south of Montes Carpathus, the southern boundary of the Imbrium basin, and 150 km north of the mapped edge of the ejecta deposit. The formation in this area is estimated to be about 500 m (meters) thick (Eggleton, 1963). The principal objective of Apollo 14 was to sample the Fra Mauro Formation in the area immediately west of Cone crater, a young blocky crater superposed on a ridge of the formation (fig. 2). Cone crater was presumed to have excavated Fra Mauro material from beneath the local regolith, making about

the upper 75 m of the formation accessible to sampling, description, and photography.

Results of the preliminary geologic investigations of the site (Swann and Field Geology Team, 1971) and of the preliminary examination of samples (Lunar Sample Preliminary Examination Team, 1971) have been published. This paper (1) presents a general report on the petrology and petrography of the Apollo 14 samples, based on our examination of the textures and structures of the rocks in hand specimen and thin section, (2) classifies these rocks, and insofar as is possible at this time, (3) discusses the stratigraphy and origin of the Fra Mauro Formation.

Acknowledgments. — This work was done under NASA contract T–4738A. We are much indebted to J. P. Lockwood and D. J. Milton, U.S. Geological Survey, for critical review of the manuscript.

RETURNED SAMPLES

Apollo 14 returned about 43 kg (kilograms) of rock samples, of which 32[1] specimens weigh more than 50 g (grams) and 124[1] specimens weigh more than 1 g (Lunar Sample Preliminary Examination Team, 1971). These samples were collected by Astronauts Mitchell and Shepard during two traverses covering a distance of about 3,175 m (Swann and Field Geology Team, 1971). The location of samples along the traverses is known for the majority of rocks; two rocks bigger than 50 g (14303, 14169) are still only tentatively located (Sutton and others, 1971).

In contrast to rocks returned by Apollo 11 and 12, the Apollo 14 rocks are predominantly fragmental and consist of clasts (>1 mm) (millimeter) and microclasts (0.1–1.0 mm) in fine-grained matrices. Indeed, only two of the 32 rocks weighing more than 50 g and a correspondingly small proportion of the 124 rocks weighing more than 1 g are homogeneous crystalline rocks (Lunar Sample Preliminary Examination Team, 1971). The homogeneous crystalline rocks all have their counterparts as clasts in fragmental rocks (Lunar Sample Preliminary Examination Team, 1971). One sample (14053) was collected from the side of a boulder, and surface descriptions by the Apollo 14 crew indicate that it was a clast in a fragmental rock (Sutton and others, 1971). The other (14310) is considerably smaller than the largest clast observed in surface photographs and is lithologically identical to clasts in returned fragmental rocks. It appears likely, therefore, that all the homogeneous crystalline rocks are clasts that were dislodged from fragmental rocks, either on the lunar surface by natural processes or by handling after collection.

[1]Totals combine samples that were broken by handling but that were given different Lunar Receiving Laboratory numbers (Swann and Field Geology Team, 1971).

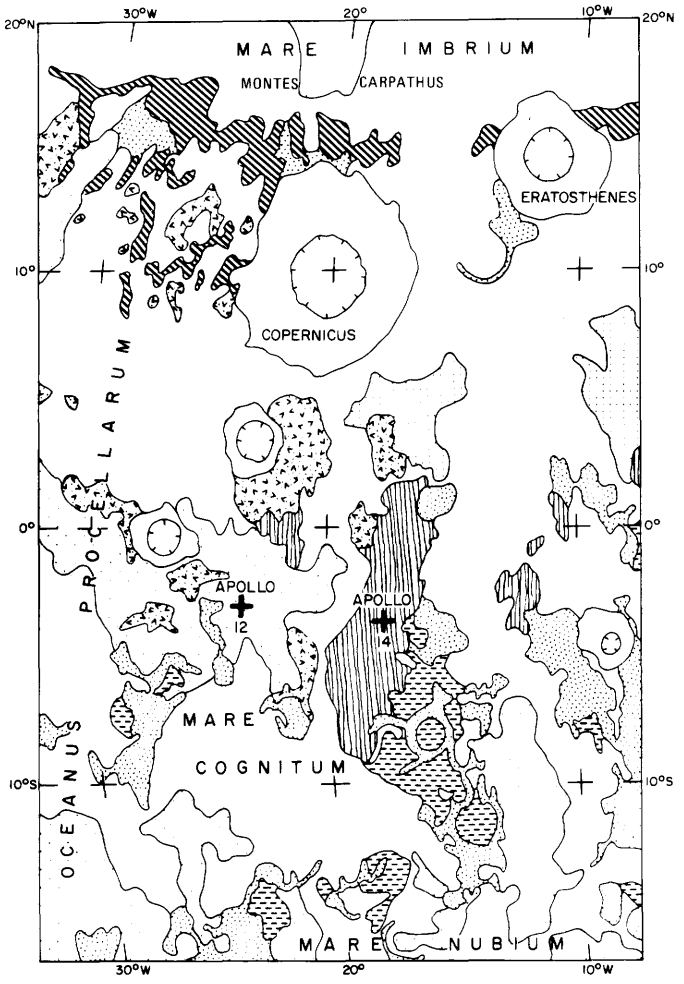

FIGURE 1. — Regional geologic map of the area surrounding the Apollo landing site. From Swann and Field Geology Team (1971).

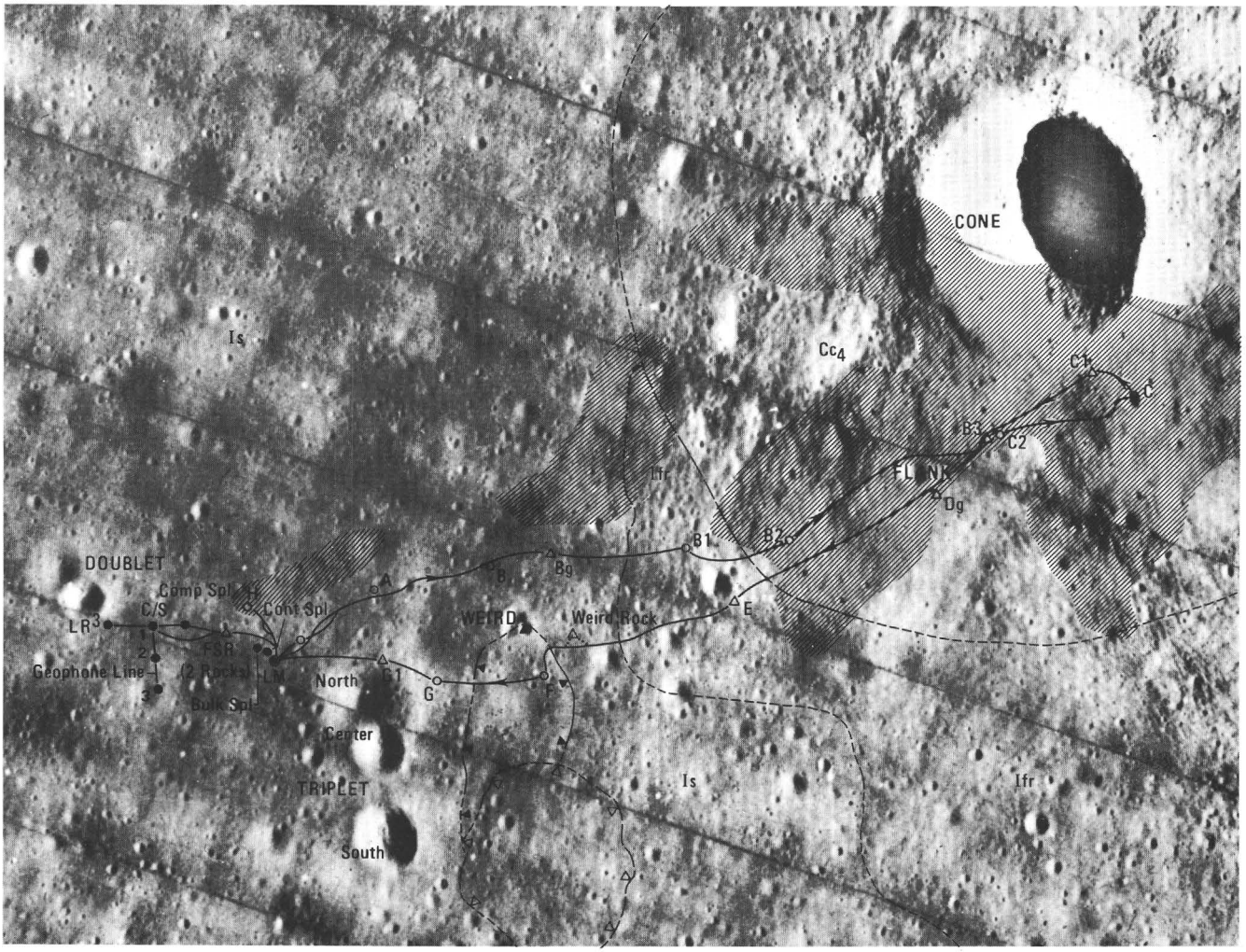

EXPLANATION

Cc_4 — Continuous ejecta blanket

Boulder ray deposits

Material of Cone Crater

Is — Smooth terrain material of the Fra Mauro Formation

Ifr — Ridge material of the Fra Mauro Formation

Contact
Long dashed where approximately located; short dashed where location is inferred without local evidence

Foot of scarp
Bounds small mesa. Short dashed where location inferred. Triangles point down slope

Edge of hill
Long dashed where approximately located; short dashed where location inferred. Triangles point down slope

Traverse route for EVA's 1 and 2

Stations
- oB – Panorama station
- △G1 – Station without panorama
- C/S – ALSEP Central Station
- LR3 – Laser Ranging Retroreflector

Samples
- FSR – Football size rock
- ●Cont Spl – Contingency sample
- ●Comp Spl – Comprehensive sample
- Dg – Grab sample at Station D

FIGURE 2. — Map of major geologic features in the Apollo 14 traverse area. From Swann, Trask, Hait, and Sutton (1971).

MEGASCOPIC STRUCTURES

Swann and Field Geology Team (1971) and Hait (1972) provided descriptions and detailed maps of the internal structures in some large boulders photographed by the astronauts. The main types of megascopic structures, besides the obvious fragmental textures, are fractures, color layering, lineation or foliation, and veins. The fractures occur in multiple sets of generally planar, parallel joints spaced from a few millimeters to a few centimeters apart. Color layering is particularly well developed in boulders from the area near the "white rocks" (fig. 3*A*), where prominent white-gray layers about 1 m thick occur. In places, soft layers are etched into depressions, presumably by micrometeorite scrubbing, while adjacent harder layers stand out as ribs. Some layering in essentially monotoned boulders is defined by differences in sizes of clasts from layer to layer; size layering also accompanies the color layering. Some layers have highly irregular contacts, whereas others are nearly plane parallel. There appear to be sizable discordances in attitude between sets of layers within two boulders (Hait, 1972), and in places, layers are contorted. Rarely, a weak lineation or, more probably, foliation is produced by alinement of lenticular clasts, and one irregular white layer about 1 cm (centimeter) thick in Weird Rock (Swann and Field Geology Team, 1971) may be a vein.

Features of this kind are, of course, less obvious in the smaller returned hand samples. Many rocks, including 14304, 14302–14305, 14312, and 14313 have shapes partly controlled by fracture sets, and a number, including 14306 and 14316, are cut by glassy veins. Sample 14082, collected from one of the "white rocks," is layered (fig. 3*B*, *C*) with millimeter- to centimeter-thick irregular units differentiated by the abundance of darker clasts and by average size of debris in the matrix (fig. 3*C*). Samples 14076 and 14453 are also layered fragmental rocks. Sample 14076 has an irregular but sharp contact separating rock with about 30 percent clasts from rock with 5 percent of the same types of clasts. Sample 14453 consists of light- and dark-colored laminae of fragmental material interlayered on a scale of 1–3 mm.

HAND-SPECIMEN PETROLOGY

One of us (Jackson) was a member of the Apollo 14 Lunar Sample Preliminary Examination Team (LSPET); the other (Wilshire) was a representative of the Apollo 14 Lunar Geology Investigation Group to the LSPET. Together, we had the opportunity to examine 107 Apollo 14 hand samples larger than 1 g, mostly with the aid of binocular microscopes. Many of our descriptions were systematized by using a form that required notation of a wide variety of features

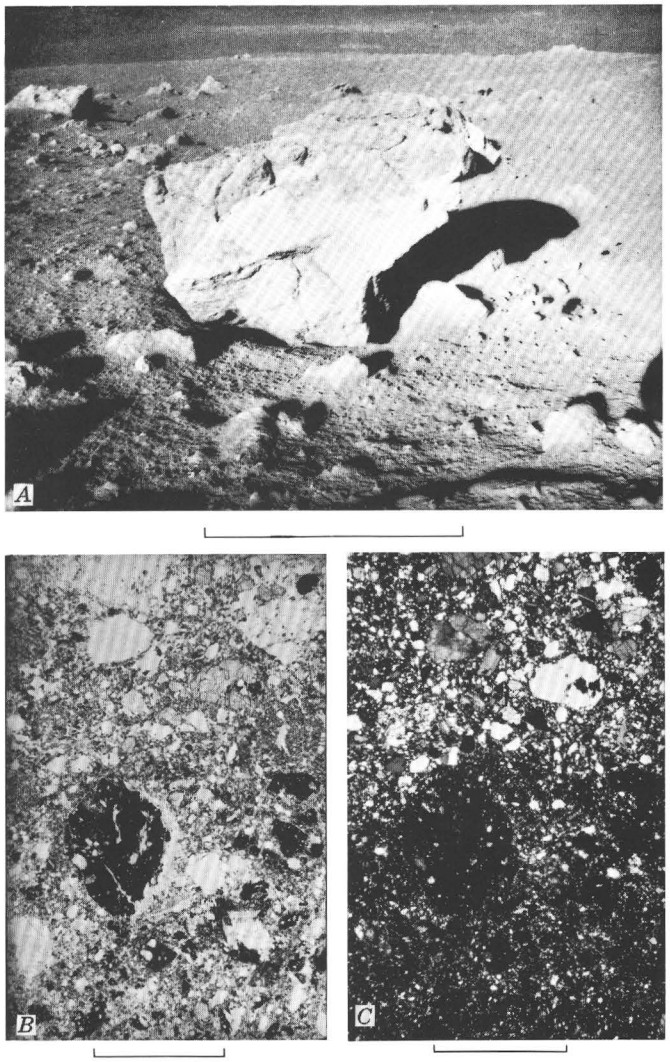

FIGURE 3. — Surface photograph and photomicrographs of Apollo 14 rocks. *A*, NASA photograph AS14–68–9448 showing complexly interlayered light and dark rocks in block near rim of Cone crater. Both rock types appear to be fragmental. Bar scale 2 m long. *B*, Photomicrograph of layering in sample 14082,11. Plane polarized light view showing planar contact between a layer lacking dark clasts and one containing them. Bar scale 1 mm long. *C*, Same area as 3*B*, crossed nicols. Layer lacking dark clasts has a coarser grained matrix. Bar scale 1 mm long.

for each specimen. Structures, textures, and lithologic properties, such as degree of induration, grain size, and mineral proportions, were systematically described and measured. This information is presented here because wide access to the hand specimens is no longer possible and because the broad petrologic framework required for classification and stratigraphic studies could not otherwise be established.

The Apollo 14 rocks may be divided into two broad groups (fig. 4): relatively homogeneous crystalline rocks and fragmental rocks (or breccias). Both groups

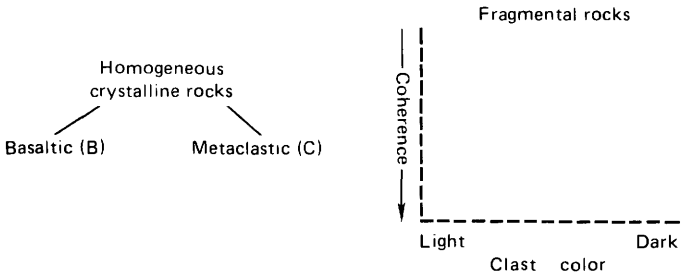

FIGURE 4. — Scheme used for subdivision of Apollo 14 rocks.

have been subdivided on the basis of megascopic features described below. In table 1, all specimens weighing more than 1 g have been classified into one of six categories — two groups (B, C) representing subdivision of the crystalline rocks, and four (F_1–F_4) representing subdivisions of the fragmental rocks.

HOMOGENEOUS CRYSTALLINE ROCKS

Group B (basaltic) rocks are even grained and aphyric, with textures ranging from intersertal to ophitic. Grain size varies from fine to medium, but most are conspicuously coarser than the metaclastic rocks. Two groups are recognized, one having about 40–50 percent plagioclase (14053, 14071, 14074) and the other having about 60–70 percent plagioclase (14073, 14078, 14079, 14276, 14310). Rock 14310 has small cognate inclusions that are mainly finer grained than the body of the rock but are modally similar to it (Melson and others, 1972). Clasts of basaltic rocks are widespread though not abundant in the fragmental rocks. Most of these rocks are richer in plagioclase, poorer in ilmenite, and have much lighter colored pyroxenes than the basaltic rocks returned by Apollo 11 and 12.

Group C (metaclastic) rocks have granular textures and are fine grained to aphanitic. The rocks are typically inequigranular, with 1–5 percent of irregular large mineral grains, usually plagioclase, but less commonly olivine or pyroxene. Both light and dark rocks of this type are very common as clasts in the fragmental rocks. All but two rocks in this group are light colored and consist principally of plagioclase and light-gray pyroxene. The two dark rocks (14006, 14440) are aphanitic and of unknown mineral composition. These rocks are similar to the common breccia clasts.

FRAGMENTAL ROCKS

The fragmental rocks, like the crystalline rocks, are distinctly different from those returned by the Apollo 11 and 12 missions. Most are coherent, contain less glass, and have larger and more abundant clasts than the fragmental rocks of earlier missions, but a few are more friable and contain fewer and smaller clasts than most Apollo 11 and 12 breccias. We have distinguished four groups of fragmental rocks on the basis of proportions of light and dark lithic fragments and matrix coherence. All four groups of fragmental rocks are polymict and contain clasts ranging in shape from angular to subrounded.

Group F_1 rocks are defined as fragmental rocks containing leucocratic lithic clasts in excess of mesocratic

TABLE 1. — *Classification of rocks larger than 1 gram*[1]

(B) Homogeneous crystalline rocks, basaltic

Sample No.			
14053	14073	14078	14276
14071	14074	14079	14310
14072			

(C) Homogeneous crystalline rocks, metaclastic

Sample No.			
14006	14077	14434	14444
14068	14274	14436	14451
14069	14429	14440	
14070	14431	14443	

(F_1) Fragmental rocks, light clasts dominant, matrix friable

Sample No.	Percent clasts >1 mm	Sample No.	Percent clasts >1 mm	Sample No.	Percent clasts >1 mm	Sample No.	Percent clasts >1 mm
14041*	2	14056	2	14177	1	14427	1
14042*	10	14057	1	14178	10	14432	2
14043*	?	14058	20	14185	?	14437	1
14045*	1	14059	1	14250	10	14438	1
14047	3	14061	?	14251	1	14442	1
14049	1	14062	1	14282	1	14449	10
14055	5	14080	1	14286	5	14452	1

(F_2) Fragmental rocks, light clasts dominant, matrix coherent to moderately coherent

Sample No.	Percent clasts >1 mm	Sample No.	Percent clasts >1 mm	Sample No.	Percent clasts >1 mm	Sample No.	Percent clasts >1 mm
14007	25	14269	10	14281	40	14315	20
14051?	1	14271	1	14285	10	14316	20
14195	1	14272	1	14288	25	14317	10
14201	10	14273	1	14294	10	14318	30
14255	2	14275	10	14297	10	14430	20
14265	10	14277	10	14301	18	14453	1
14267	10	14278	20	14307	20		
14268	10	14280	40	14313	5		

(F_3) Fragmental rocks, dark clasts dominant, matrix friable

Sample No.	Percent clasts >1 mm	Sample No.	Percent clasts >1 mm	Sample No.	Percent clasts >1 mm	Sample No.	Percent clasts >1 mm
14063	23	14082*	10	14171	30	14426	5
14064	40	14083*	15	14196	10		

(F_4) Fragmental rocks, dark clasts dominant, matrix coherent to moderately coherent

Sample No.	Percent clasts >1 mm	Sample No.	Percent clasts >1 mm	Sample No.	Percent clasts >1 mm	Sample No.	Percent clasts >1 mm
14066	25	14179	20	14266	25	14308*	20
14075	5	14180	1	14270	?	14309	20
14076	5	14181	50	14279	1	14311*	20
14169	25	14182	5	14296	15	14312	45
14170	5	14188	5	14302*	28	14314	25
14172	6	14194	8	14303	28	14319	35
14173	20	14197	20	14304	25	14320	13
14174	10	14199	20	14305*	28	14321	30
14175	1	14264	10	14306	15	14445	15
14176	1						

Samples lacking sufficient information for certain classification

Sample No.	Tentative identification
14008	F_1
14060	F_1
14198	B

*Identifies broken pieces of same sample: 14041, 14042, 14043, 14045 parts of same sample; 14302, 14305 parts of same rock; 14308, 14311 parts of same rock; 14082, 14083 parts of same rock.

[1]For location see Swann and Field Geology Team (1971); for weight see Apollo 14 lunar sample information catalog, NASA TMX-58062.

and melanocratic lithic clasts and having friable matrices. There are 25 rocks in this category ranging in weight from 1.5 to 242 g (table 1). In more than half of these rocks, leucocratic clasts make up more than 90 percent of total number of clasts larger than 1 mm.[2] The abundance of clasts in these rocks is low (fig. 5). The majority of the clasts are lithic crystalline very fine grained feldspar-rich rocks; many appear to have originally been fragmental. Angular glass fragments, broken spheres, and spheres, mostly medium brown, are common. Mineral fragments larger than 1 mm are rare. The matrices of these rocks are medium gray and, down to the limit of resolution, consist of the same materials as the clasts, but with much larger proportions of glass and mineral fragments. Many of these rocks may be weakly indurated regolith.

Group F_2 rocks are defined as fragmental rocks containing leucocratic clasts in excess of the total of mesocratic and melanocratic clasts and having moderately coherent to coherent matrices. There are 30 rocks in this category ranging in weight from 1.5 to 1,360 g (table 1). In about 60 percent of these, leucocratic clasts make up more than 90 percent of total number of lithic clasts larger than 1 mm. The abundance of clasts is much greater than in F_1 rocks (fig. 5); nearly 80 percent of F_2 rocks contain 5 percent or more clasts greater than 1 mm. The majority of the clasts are lithic, and most of them are megascopically indistinguishable from those in group F_1. Clasts of basaltic rock very similar to those of group B are present. Very fine grained melanocratic clasts that characterize groups F_3 and F_4 fragmental rocks, while never dominant, are present in many F_2 rocks. A few small clasts of finely granular nearly pure olivine and pyroxene aggregates are present in some F_2 rocks. Mineral fragments larger than 1 mm are rare, and glass clasts are distinctly less abundant than in group F_1 rocks. Matrix colors range from light to dark gray. Mineral fragments are more abundant than lithic fragments in the size fraction smaller than 1 mm.

Group F_3 and F_4 rocks are defined as fragmental rocks containing melanocratic and mesocratic fragments in excess of leucocratic clasts. The groups are further subdivided on the basis of matrix coherence: group F_3 rocks have relatively friable matrices, and F_4 rocks are moderately coherent to coherent. So defined, group F_3 contains only six rocks, all relatively small. Two of these rocks (14082, 14083), the "white rocks," appear to be unique, but 14063 and 14064 also have light-colored matrices. The "white rocks" owe their light color to the matrix material, but clasts larger than 1 mm are dominantly melanocratic. The F_4 category contains 35 rocks, the largest weighing nearly 9 kg (table 1). Clasts larger than 1 mm are abundant (fig. 5). The majority of the clasts are lithic crystalline aphanitic dark-gray to black rocks, many with metamorphic textures. Leucocratic clasts apparently like those of group F_2 are present but not dominant. Basaltic rocks similar to those of group B are present in some rocks, and clasts of granular olivine and pyroxene aggregates seem to be more abundant than in group F_2. The matrices vary in color from light to medium gray.

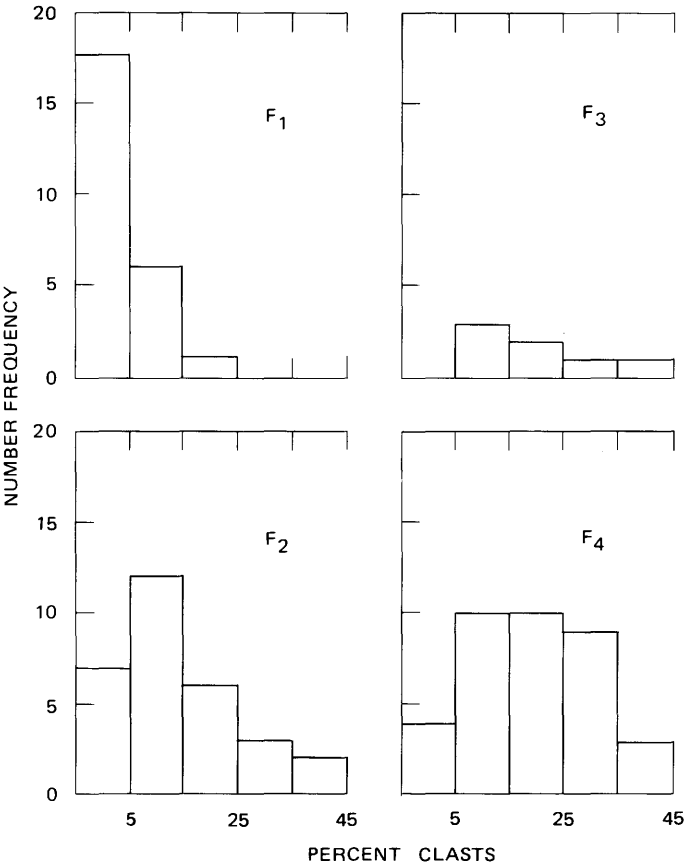

FIGURE 5. — Frequency distribution of clasts >1 mm in fragmental rocks of groups F_1, F_2, F_3, and F_4.

Almost all the samples can be classified according to the scheme described above. Among several specimens, however, that have noteworthy macroscopic features in addition to the characteristics used in the classification are glass-cemented breccias (14080, 14251, 14307), a single fragment largely composed of metal (14286), and a single small glass sphere (14425).

THIN-SECTION PETROLOGY

Thin sections of only 30 of the samples examined megascopically are available. We studied 200 thin sec-

[2]Most of the breccias have seriate fragment sizes. We arbitrarily subdivide these as "clasts," >1 mm, and "microclasts," 0.1–1.0 mm. "Matrix" refers to glass and fragmental material <1 mm.

tions of these 30 rocks. Clasts that could be identified as such in individual thin sections of fragmental rocks were divided into glass, mineral, and igneous and metamorphic lithic types. These groups were further subdivided into a total of 22 recognizable clast types and several subtypes based on mineralogy, color, and texture. (See table 2 for list of types.) The generally small size of the thin sections often did not allow good statistical results to be obtained for clasts larger than 1 mm. Accordingly, counts were also made of fragmental material in the size range 0.1–1.0 mm, which we refer to here as "microclasts." Systematic microscopic descriptions and counts of clast types of 19 different fragmental rocks were made from 89 thin sections. Counts of 100 clasts and microclasts were generally made, although for some samples as many as 215 were systematically described and for others the lack of thin sections resulted in counts of as few as 15. A total of more than 3,000 clasts and their individual dimensions were thus identified. The results of these clast counts are given below.

TABLE 2. — *Principal types of clasts and microclasts*

Identifying symbols	*Clast-microclast type*
A_1	Pale-yellow to brown glass.
A_2	Colorless glass.
B_1	Plagioclase.
B_2	Clinopyroxene.
B_3	Olivine.
B_4	Orthopyroxene.
B_5	Opaque minerals.
C_1	Intersertal basalt.
C_2	Ophitic basalt.
C_3	Intergranular basalt.
C_4	Variolitic basalt.
C_5	Vitrophyric basalt.
C_6	Graphic quartz-alkali feldspar.
C_7	Plagioclase, orthopyroxene cumulates.
C_8	Hypautomorphic gabbro, norite.
D_1	Recrystallized plagioclase.
D_2	Light-colored metaclastic rock.
D_3	Metabasalt.
D_4	Dark-colored metaclastic rock.
D_5	Recrystallized olivine.
D_6	Recrystallized pyroxenes.
D_7	Metagabbro.

The problem of differentiating the matrices of the fragmental rock proved more difficult. In general, the finer component down to the limits of microscopic resolution consists of the same constituents as the clasts, progressively disaggregated as the grain size decreases. Much material, however, cannot be resolved optically. In some rocks, postconsolidation metamorphism has further affected the compositions and textures of the matrices (Wilshire and Jackson, 1972; Warner, 1972).

GLASS CLASTS

Two varieties of glass clasts (class A, table 2) were distinguished optically: (1) pale-yellow to dark-brown glass that usually contains mineral and lithic debris and that commonly contains newly formed crystallites (type A_1); and colorless glass lacking both inclusions of rock debris and crystallites (A_2). Glass clasts (>1 mm) are proportionally less abundant than microclasts (0.1–1.0 mm) in the total clast population (fig. 6). Most glass clasts and microclasts are irregular, angular fragments that were clearly solid when incorporated in the fragmental rocks. Some, however, have shapes suggesting that they were soft and were deformed during their incorporation. Spheres and pieces of spheres of both yellow-brown and colorless glass occur sparsely. The colorless glass may largely be shocked plagioclase (maskelynite); the more common colored glasses probably have the wide range of basaltic compositions reported for glasses in Apollo 14 soils (Jakeš and Reid, 1971; McKay and others, 1972; Chao and others, 1972; Carr and Meyer, 1972).

MINERAL CLASTS

Mineral fragments (class B, table 2) make up a sizable proportion of microclasts in all the fragmental rocks but, as might be expected, are proportionally more abundant in the 0.1- to 1.0-mm-size fraction than in the >1.0 mm fraction (fig. 6). A small percentage, however, attain sizes as large as 2.5 mm. Plagioclase (B_1) is clearly the dominant mineral clast (fig. 6), but proportions of pyroxene are as much as 50 percent (fig. 7). A few plagioclase grains appear to have been compositionally zoned along irregular boundaries and subsequently broken across the zones. Pyroxene clasts include pale-brown to colorless augite (B_2), nearly colorless pyroxene with low birefringence and inclined extinction (presumed to be pigeonite, but not differentiated from augite in the counts), and orthopyroxene (B_4). Orthopyroxene clasts, especially the large ones, commonly contain exsolution lamellae of clinopyroxene (Papike and Bence, 1971); the clinopyroxenes are commonly, but not always, slightly more abundant than the orthopyroxene (fig. 6). Olivine (B_3) is present sparsely as mineral clasts as large as 2.3 mm. Optical properties and preliminary electron microprobe data indicate that it is typically very magnesian.

Minor constituents of the mineral microclast fraction (B_5) include ilmenite, metallic iron, troilite, chromian spinel, ulvöspinel, native copper, armalcolite, zircon, apatite, and potassium feldspar(?) (Lunar Sample Preliminary Examination Team, 1971). In addition, we have observed quartz and a dark-green

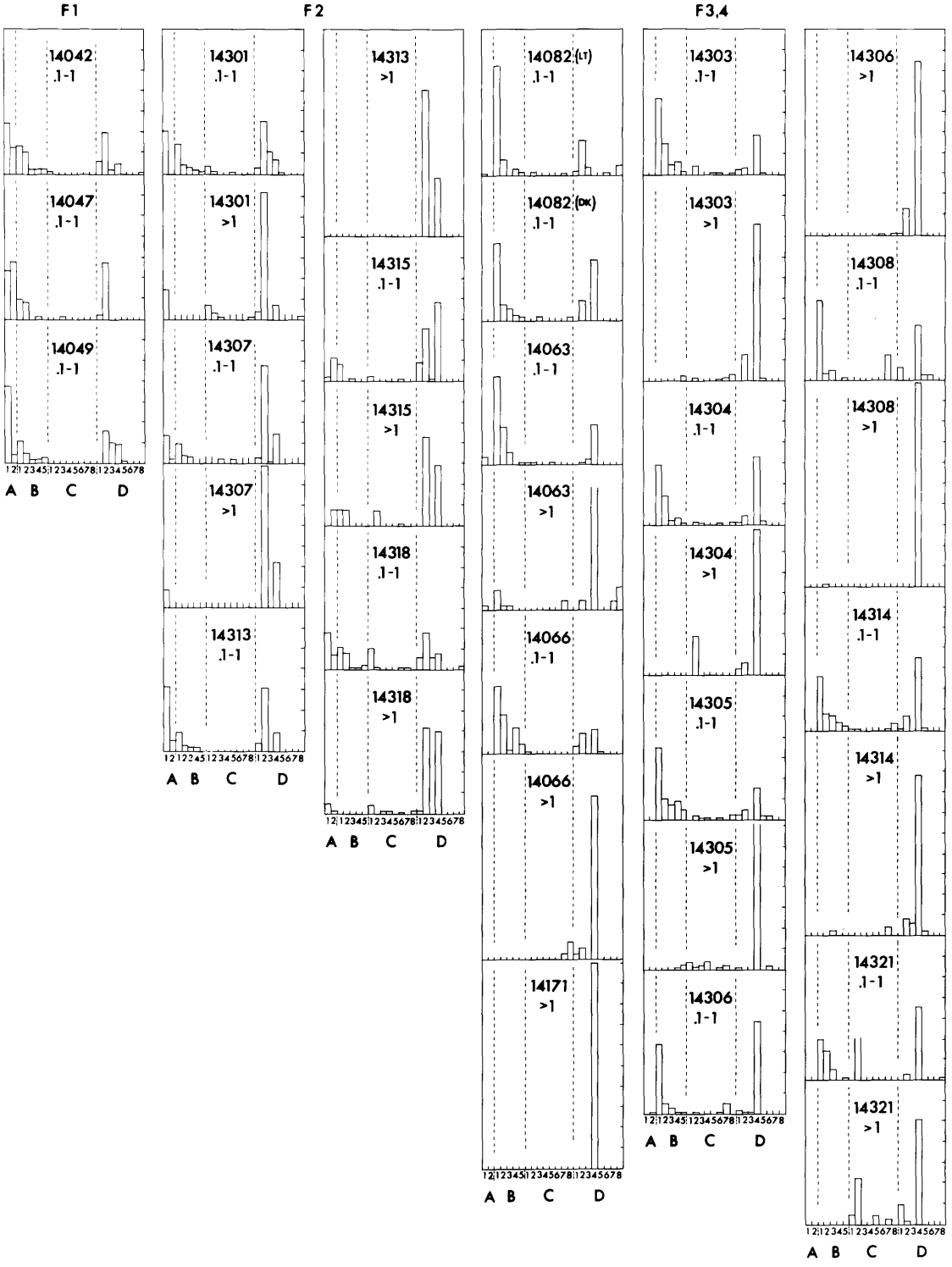

FIGURE 6. — Histograms showing relative abundance of glass (A), mineral (B), igneous (C), and metamorphic (D) clasts (>1 mm) and microclasts (0.1–1.0 mm) in the fragmental rocks of groups F_1, F_2, F_3, and F_4.

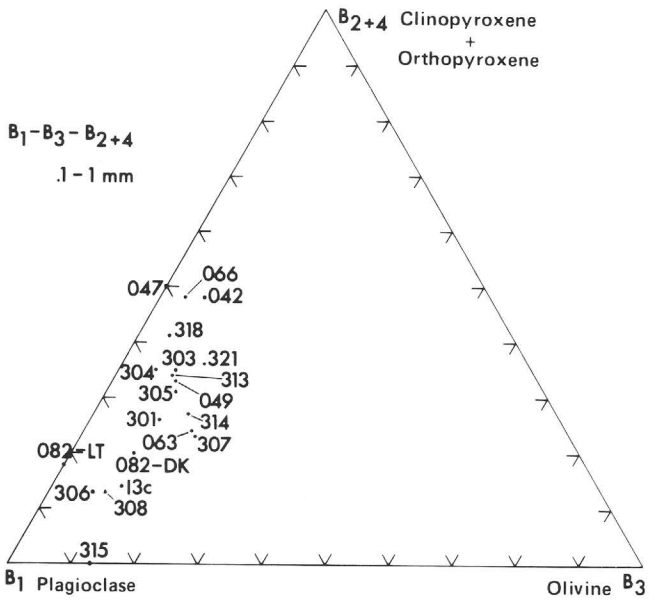

FIGURE 7. — Triangular plot of plagioclase(B_1)-pyroxene-(B_2+B_4)-olivine(B_3) microclasts.

amphibole(?) (thin section 14308,2) in some thin sections.

LITHIC CLASTS

IGNEOUS ROCKS

Nine varieties of igneous rocks occur as clasts and microclasts (table 2): five textural variants of largely crystalline basalt, vitrophyric basalt (five subtypes), graphic intergrowths of quartz and alkali feldspar, cumulates (seven subtypes), and hypautomorphic-granular rocks (two subtypes). Despite the considerable variety of lithologies, clasts of igneous rock are not particularly abundant among the lithic clasts as a whole (fig. 6).

The most abundant igneous rock type is aphyric intersertal basalt (C_1). Clast sizes in thin section are as large as 6 mm (table 3), but rock 14310, inferred to be a clast, is of this type and measures about 18 cm (centimeters) across. The majority of these rocks are somewhat finer grained than 14310, but 14310 is texturally inhomogeneous (Ridley and others, 1971; Melson and others, 1972) on a scale comparable to or larger than the average clast size of the basalts (fig. 8*A*). Rocks with intersertal texture are rich in plagioclase (table 4), which typically forms slender euhedral crystals interspersed with subhedral clinopyroxene. Opaque minerals (ilmenite, troilite, metallic iron) are present in small amounts (table 4). The groundmass, ranging from about 1 to 40 percent, is composed partly of very fine grained apatite(?), ilmenite, troilite, alkali feldspar(?), glass, and unidentified minerals (Lunar Sample Preliminary Examination Team, 1971). It is possible that sample 14310 and similar clasts are products of near-surface rocks that were shock melted (Dence and others, 1972).

TABLE 3. — *Clast sizes and grain sizes of some igneous clasts*

Group (table 2)	Maximum clast size in thin section (mm)	Average grain size (mm)
C_1	6	0.03–0.08
C_2	5	.1 – .2
C_3	4	.05
C_4	4	
C_5	4	.1 – .2
C_6	2	.5 – .6
C_7	2	.05– .13
C_8	7.5	.2 –3.0

TABLE 4. — *Modal compositions of basalts, in volume percent*

[Tr., trace]

	Intersertal					Ophitic				Intergranular	
Plagioclase	60	55	60	58	70	55	40	50	50	80	50
Pyroxene	30	35	....	30	19	39	58	45	45	10	50
Olivine	....	....	....	....	1	5	1	5	5	2	....
Opaque	Tr.	Tr.	1	2	Tr.	1	1	....	....	8	....
Mesostasis	10	10	39	10	10	....	....	....	....	....	....

Aphyric basalt clasts and microclasts with ophitic texture (C_2) are almost as abundant as intersertal basalts, and the two types may intergrade. In rock 14310, intersertal texture tends to grade toward ophitic or subophitic texture as the grain size increases. This group of clasts differs from the ophitic parts of 14310 mainly in having a small percentage of olivine. Clast sizes in thin section are as large as 5 mm, but the largest C_2 clast returned is sample 14053. Average grain sizes are somewhat coarser than those of C_1 rocks (table 3), as large as 0.6 mm in rock 14053 (Melson and others, 1972). These rocks typically have lower plagioclase contents (40–50 percent) than intersertal basalts (table 3), probably in part due to nonrepresentative sampling of small clasts. Plagioclase forms euhedral grains that penetrate larger anhedral to subhedral pyroxenes (fig. 8*B*). Olivine occurs sparsely, usually as ragged grains in cores of pyroxenes. Opaque minerals (metallic iron, ilmenite, troilite) are not abundant (table 3). Tridymite and cristobalite occur in interstices and vugs of some rocks, and some rocks contain 1 percent or less of interstitial material (including metallic iron, dendritic ilmenite, fayalite(?), and glass (Lunar Sample Preliminary Examination Team, 1971).


A

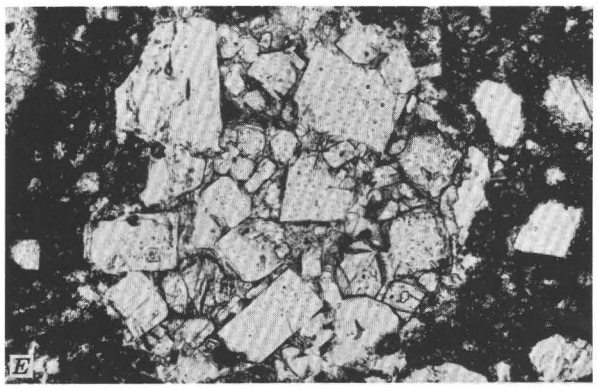
E


B

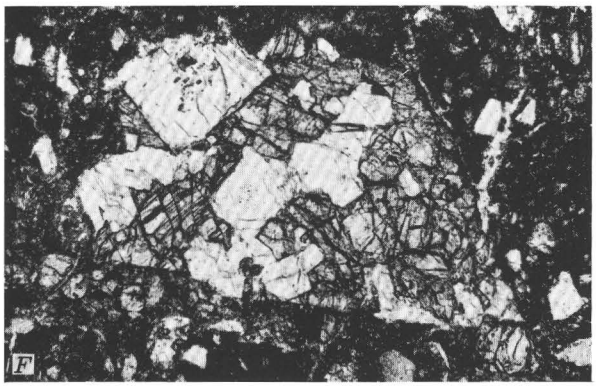
F

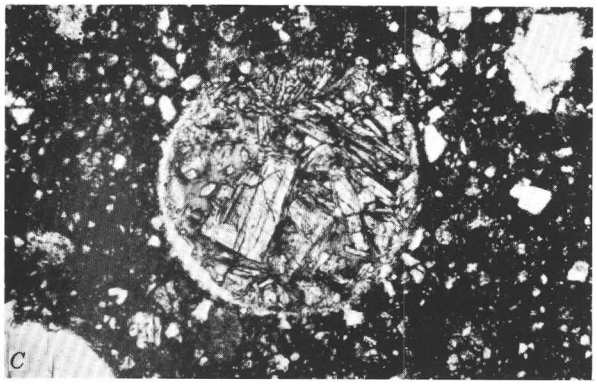
C

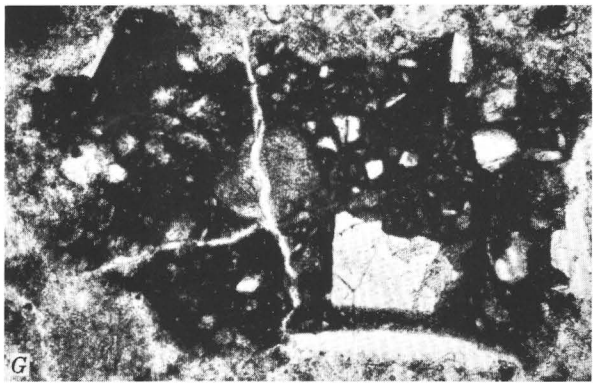
G

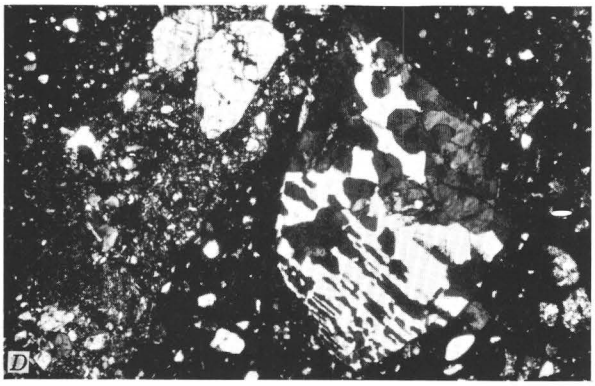
D

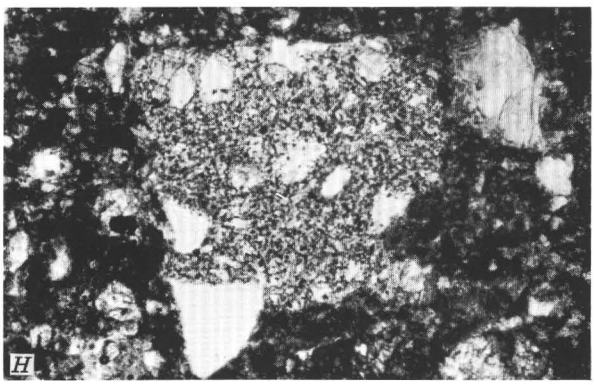
H

Clasts of basaltic rock with intergranular (C_3) and variolitic (C_4) texture are moderately widespread (fig. 6) but are not abundant. Modes are given in table 4, size data in table 3.

Clasts of basaltic rock with vitrophyric texture (C_5) have been found in thin sections of seven rocks (fig. 6). These clasts are as large as 4 mm (table 3) and either are irregular angular to subangular fragments or have nearly perfectly circular cross sections (fig. 8*C*). The circular ones are among the features called chondrulelike by King, Butler, and Carman (1971, 1972) and by Fredriksson, Nelen, Noonan, and Kraut (1972). Five subtypes, all containing very dark brown glass, were identified on the basis of their mineralogy (table 5).

TABLE 5. — *Types of vitrophyres*

Group	*Crystal phases*
C_{5a}	Plagioclase only.
C_{5b}	Olivine only.
C_{5c}	Plagioclase, olivine.
C_{5d}	Plagioclase, clinopyroxene.
C_{5e}	Plagioclase, olivine, clinopyroxene.

Clasts of graphic to irregular intergrowths of alkali feldspar and quartz (C_6) are widespread but not abundant. Irregular quartz grains are intergrown with larger (table 3) alkali feldspar grains (fig. 8*D*). In places irregular blades of quartz that are comparable in one dimension to the alkali feldspar are intergrown with alkali feldspar.

FIGURE 8. — Photomicrographs of Apollo 14 rocks. *A*, Photomicrograph of fine-grained cognate inclusion (upper left ⅓ of photograph) in 14310,10. Boundary with normal rock is gradational, and both parts are composed of plagioclase laths, pyroxene, a trace of opaque minerals, and fine-grained interstitial material. *B*, Photomicrograph of ophitic basalt, 14053,6. Plagioclase laths penetrate zoned pigeonitic pyroxenes. Opaque minerals and olivine are scarce. *C*, Photomicrograph of a round clast of vitrophyre composed of skeletal olivine prisms and a small amount of plagioclase in finely devitrified glass. 14318,8. *D*, Photomicrograph of a clast that consists of a graphic intergrowth of quartz and alkali feldspar. 14318,8. *E*, Photomicrograph of a cumulus clast composed of euhedral cumulus plagioclase and orthopyroxene (higher relief than the plagioclase) in a groundmass of finer grained postcumulus plagioclase, pyroxene, opaque minerals, and glass. 14321,29. *F*, Photomicrograph of a cumulus clast composed of euhedral cumulus plagioclase with postcumulus clinopyroxene. 14171,13. *G*, Photomicrograph of a dark aphanitic (D_4) metaclastic clast composed of porphyroclastic plagioclase and a finely recrystallized plagioclase clast (D_1) near center, in a dark microcrystalline matrix. 14063,28. *H*, Photomicrograph of a light-colored (D_2) metaclastic rock with plagioclase porphyroclasts in a moderately coarse grained granoblastic matrix composed of plagioclase, orthopyroxene, and opaque minerals. 14042,7. Bar scale 0.5 mm long.

Rocks with cumulus textures (C_7) are among the most widespread igneous clasts (fig. 6), though they are not as abundant as either intersertal or ophitic basalts. They are typically subangular to subrounded and are as much as 2.0 mm in size (table 3). Seven varieties of cumulates are identified on the basis of types of cumulus and postcumulus phases (table 6).

TABLE 6. — *Modes and average grain sizes of common cumulates*

Cumulus minerals (volume percent)	Postcumulus phases	Average cumulus grain size (mm)
Plagioclase (45)	Orthopyroxene (55) Opaque (trace)	0.05
Clinopyroxene and olivine (42)	Plagioclase (58) Opaque (trace)	0.05–0.07
Plagioclase (37) Orthopyroxene (13)	Plagioclase (27) Pyroxene (20) Glass (3)	0.05
Plagioclase (40)	Clinopyroxene (55) Opaque (5)	0.07
Plagioclase (79) + postcumulus overgrowth (?)	Clinopyroxene (15) Glass (6) Opaque (trace)	0.13
Clinopyroxene (42)	Plagioclase (58) Opaque (trace)	0.06
Plagioclase (40) (with tiny olivine (?) inclusions)	Plagioclase Orthopyroxene Alkali feldspar Glass } (60)	0.13

The textures of these rocks vary considerably (figs. 8*E*, *F*), depending in part on the degree of postcumulus modifications in the shape of cumulus grains. Plagioclase is the dominant cumulus phase in all but one variety and is the only cumulus phase in three (table 5). Other cumulus minerals are clinopyroxene, orthopyroxene, and olivine. Postcumulus material includes plagioclase, glass, opaque minerals, clinopyroxene, orthopyroxene, and alkali feldspar.

Clasts composed of igneous rock with hypautomorphic granular textures (C_8) are moderately widespread (fig. 6). Most are subangular clasts as much as 7.5 mm in diameter (table 3). One is norite composed of about 45 percent plagioclase, 50 percent orthopyroxene, 4 percent clinopyroxene, and 1 percent opaque minerals. The other coarser clasts (table 3) are gabbros and anorthosites. Their coarse grain size suggests that small clasts will not yield representative modes.

METAMORPHIC ROCKS

Seven types of metamorphic rocks (class D, table 2) occur as clasts and microclasts in the Apollo 14 fragmental rocks: two varieties of metaclastic rocks (one dark and one light colored), metabasalts, metagabbros, and three main types of recrystallized mineral grains.

All these metamorphic rocks have some variant of hornfels texture, with relicts of angular material that suggest a premetamorphic cataclastic texture.

Metaclastic rocks are the most abundant of all clasts in the Apollo 14 fragmental rocks. They are characterized by the presence of relict angular crystal debris (porphyroclasts), ranging from a trace to 75 percent of the rock or more, in a granoblastic or poikiloblastic matrix. Plagioclase dominates as a relict mineral, but clinopyroxene, orthopyroxene, olivine, and quartz occur. Of the two varieties, the dark-colored clasts (D_4) are more abundant than the light-colored ones. D_4 metaclastic rocks are principally recrystallized cataclasite and ultracataclasite (Spry, 1969), which are dark both in hand specimen and in thin section (table 2; fig. 8*G*). Clast sizes in thin section are as large as 8.0 mm. Though there appears to be a gradation in this class from extremely fine grained very dark rocks to somewhat coarser lighter gray rocks, some breccias (for example, 14306, 14063, 14312, 14171) have distinct clasts at both ends of the spectrum, with few intermediate individuals. In places, these contrasting types are interbanded, and in others, one type may occur as clasts in the other. Even the coarsest grained rocks of this type are too fine grained to enable identification of most minerals, but they appear to have a higher opaque-mineral content than the light-colored metaclastic rocks, and the pyroxenes appear to be principally clinopyroxene. Some of these clasts show evidence of having been partly fused (buchite), and small amounts of glass have, in a few samples, survived recrystallization. In others, the original presence of a melt is indicated by occurrence of vesicles and of small microlites of olivine or plagioclase along with the coarser porphyroclasts.

A second common variety of recrystallized cataclasites (D_2) are light colored in hand specimen and in thin section (table 2). These rocks are generally coarser grained than the dark metaclastic rocks, and they are characterized by granoblastic or poikiloblastic textures. Granoblastic textures (fig. 8*H*) tend to become granoblastic-polygonal with increasing grain size. In rocks with poikiloblastic texture (fig. 9*A*, *B*), the host mineral (orthopyroxene or clinopyroxene) enclosing plagioclase granules ranges in size from >0.05 to 0.10 mm. Some of the more coarsely recrystallized clasts also show development of porphyroclastic plagioclase (fig. 9*C*) and growth of small lath-shaped plagioclase grains. Where such rocks lack porphyroclasts, they resemble plagioclase cumulates, except for their fine grain size. In general, however, the former fragmental nature of these rocks is clearly evidenced by their angular grains and very poor sorting. Plagioclase is clearly the dominant mineral, although its proportion is extremely variable. In the majority, orthopyroxene is the most abundant mafic mineral. Clinopyroxene occurs with the orthopyroxene in some rocks and is the only pyroxene in a few; the consistently low birefringence of the clinopyroxene suggests that it is mainly pigeonite. Opaque minerals are a constant accessory, and small amounts of porphyroclastic olivine are common.

Metabasalts with granoblastic textures (D_3) are moderately widespread but are not abundant (fig. 5). Most of these appear to have had intergranular or intersertal textures before metamorphism and now consist of a granular aggregate of augite, with or without olivine, equant opaque minerals, and ragged plagioclase that commonly tend to poikiloblastically enclose other minerals. The rocks closely resemble hornfelsed basalts in the Apollo 11 samples, described by James and Jackson (1970), though many are coarser grained. Typical modes and grain sizes are given in table 4.

The metagabbros (D_7) are not only rare, but also unusual rocks. A few of them may have been troctolites (figs. 9*D*, *E*) in which what appear to be cumulus olivine grains are distributed among plagioclase grains. Both the olivine and the plagioclase have been recrystallized to fine-grained granoblastic aggregates, but the original texture of the rock is preserved. An even more striking example is illustrated in figure 9*A* and *B*, in which original euhedral shapes of plagioclase, possibly ophitically enclosed by pyroxene, are preserved despite coarse recrystallization to a decussate mosaic.

Virtually monomineralic clasts of plagioclase or olivine hornfels are common, and similar ones of clinopyroxene and orthopyroxene occur sparsely. The clasts typically are ovoid and subround but may be blocky and angular. Their size ranges from 0.01 to 3.0 mm but averages about 0.25 mm. Grain sizes vary

FIGURE 9. — Photomicrographs of Apollo 14 rocks. *A*, Photomicrograph of a light-colored (D_2) metaclastic rock with poikiloblastic orthopyroxene enclosing small plagioclase grains. 14082,12. *B*, Same area as 9*A*. Crossed nicols. Note zoning of porphyroclastic plagioclase. *C*, Photomicrograph of a light-colored (D_2) metaclastic rock with porphyroclastic plagioclase in a coarse-grained matrix composed of orthopyroxene poikiloblastically enclosing plagioclase laths, crossed nicols. 14063,25. *D*, Photomicrograph of a "metatroctolite" composed of olivine and plagioclase. Plane polarized light. 14301,13. *E*, Same as 9*D*, crossed nicols, showing granoblastic recrystallization of both olivine and plagioclase. *F*, Photomicrograph of a "metagabbro" clast with euhedral plagioclase grains enclosed by clinopyroxene. Plane polarized light. 14270,9. *G*, Same view as 9*F*, crossed nicols, showing decussate recrystallization of the plagioclase and granoblastic texture of the pyroxene. *H*, Photomicrograph of clast with areas of a single relict plagioclase grain, crossed nicols. 14312,19. Bar scale 0.5 mm long.

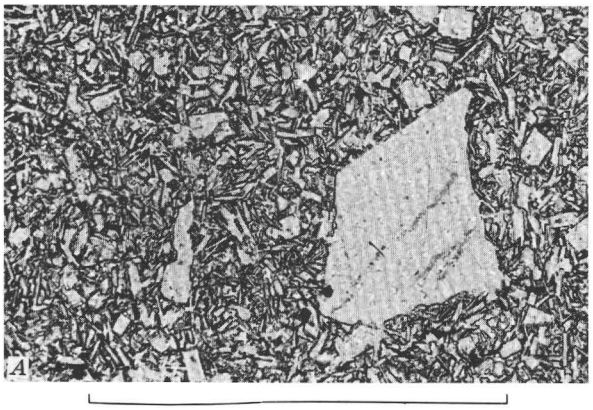
A

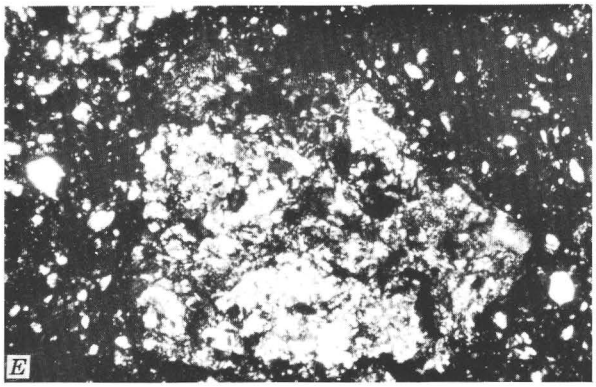
E

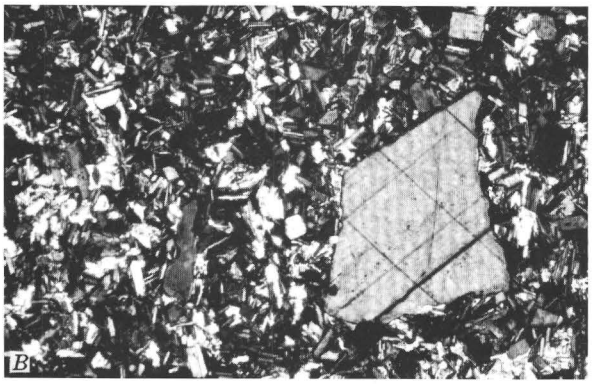
B

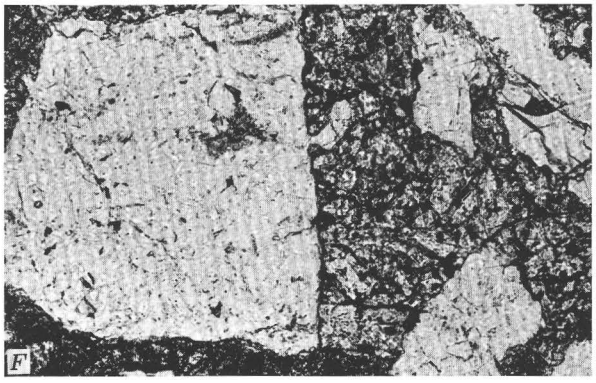
F

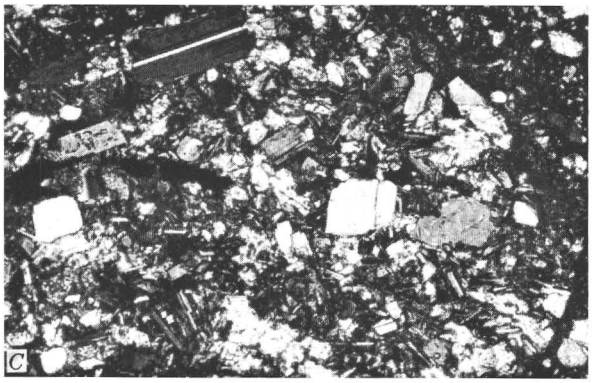
C

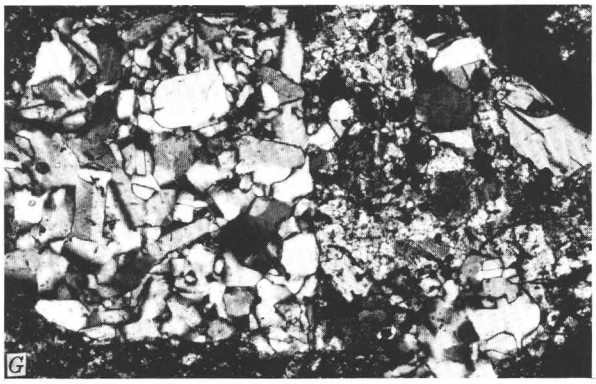
G


D

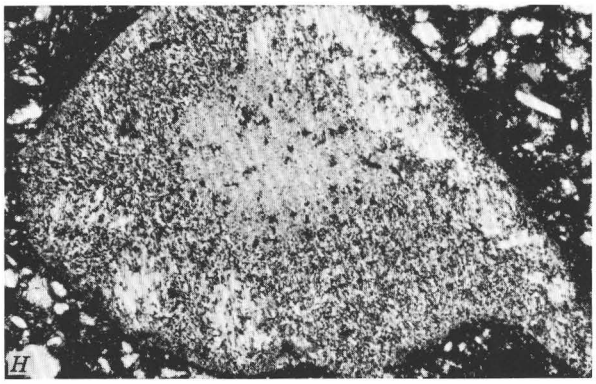
H

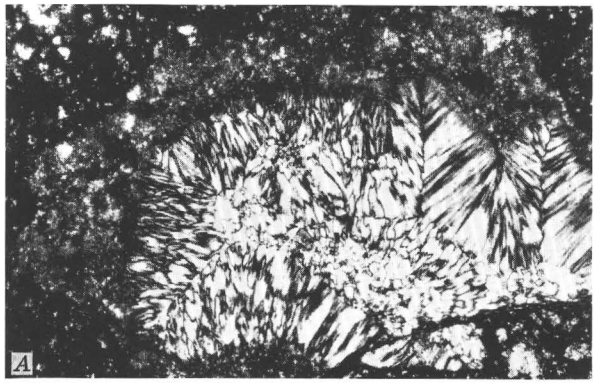
A


E

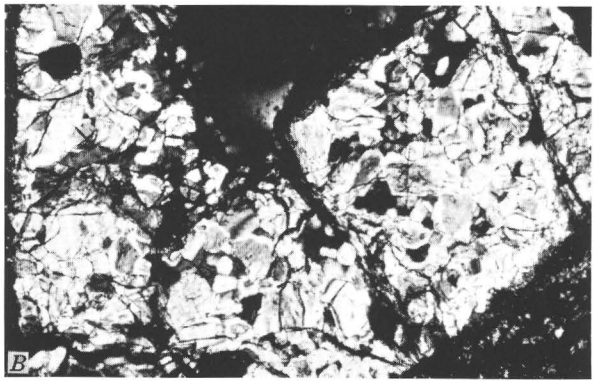
B

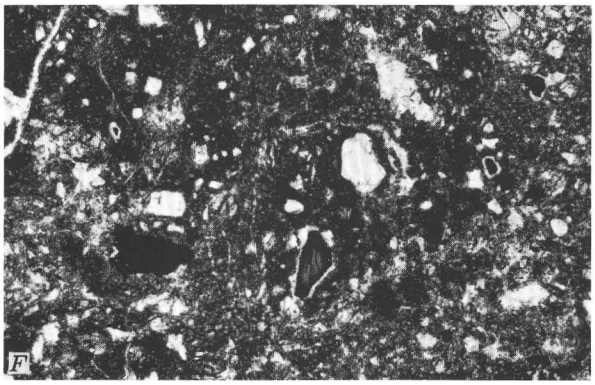
F

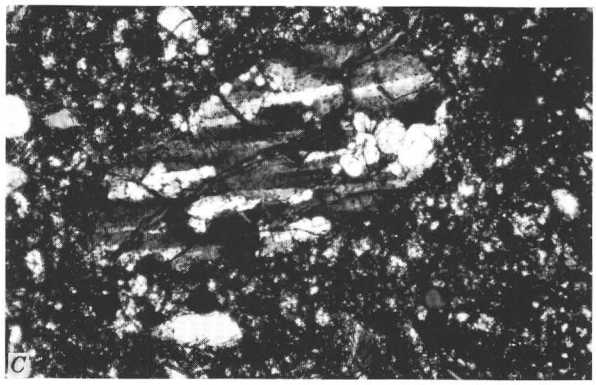
C

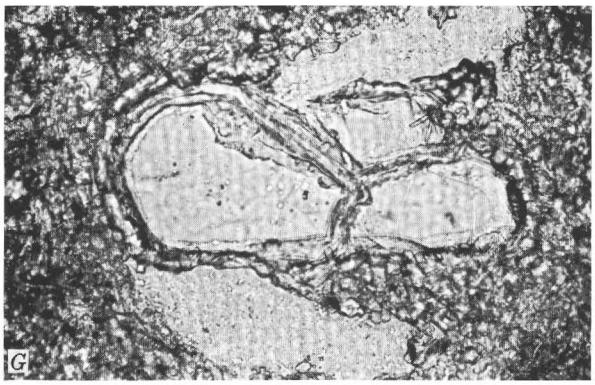
G

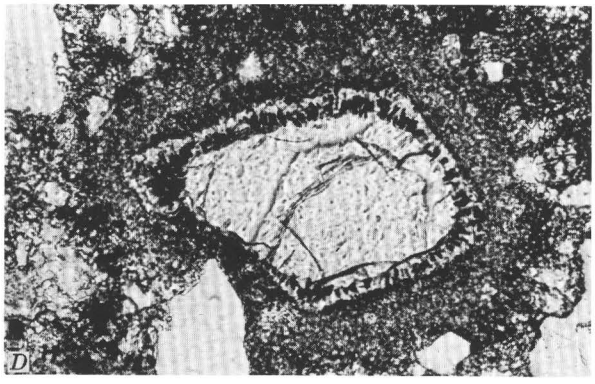
D

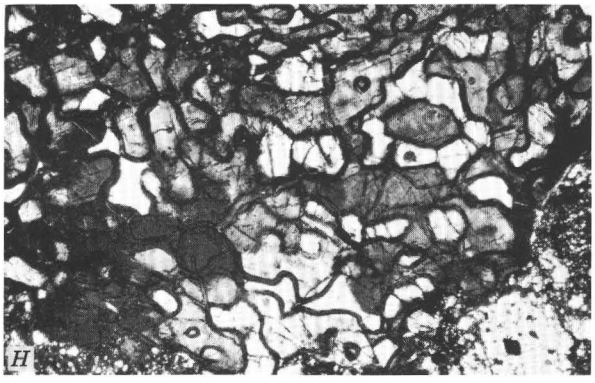
H

somewhat (range 0.03 to 0.08 mm), with typical grain sizes for the plagioclase clasts at the lower end of the range and for olivine clasts at the upper end. Plagioclase hornfels (D_1) are by far the most abundant of the monomineralic hornfels and show the widest variety of textures. Most plagioclase clasts consist of fine interlocking anhedra that are either elongate blebs or irregular in shape. Spherulitic texture in the plagioclase clasts is common and in some is spectacularly developed (fig. 10*A*). A few plagioclase clasts have granoblastic-polygonal textures that closely resemble those in Apollo 11 rocks described by Wood, Dickey, Marvin, and Powell (1970a, b), and others have striking decussate textures resembling the feldspar in metagabbro clasts. Olivine hornfels (D_5) typically have granoblastic-polygonal textures (fig. 10*B*) and are composed of interlocking grains of undeformed olivine. Pyroxene hornfels (D_6) are uncommon, and those composed of orthopyroxene are especially rare. Both have granoblastic-polygonal textures.

Relicts of the mineral grains that recrystallized to hornfels are present in a number of these clasts; no polycrystalline relicts of mafic silicates were observed, the unrecrystallized material in all samples being relicts of a large single grain (fig. 10*C*). However, a few incompletely recrystallized plagioclase clasts have relicts that suggest a polycrystalline source, and we cannot be sure that we have not counted some previously polygranular plagioclase aggregates in this group. It is nevertheless clear that the great majority of these monomineralic aggregates are recrystallized single crystals. It is possible that they were formed from disaggregated coarse-grained metagabbros like those illustrated in figure 9 (*D–G*). Ave'Lallement and Carter (1972) attributed the conditions of recrystallization to shock processes. However, we have observed olivine with a similar texture in an unshocked olivine pyroxenite inclusion in basalt from Kilbourne's Hole, N. Mex. Also, Wilson (1969) described recrystallization of pyroxene in granular aggregates in terrestrial granulites without modification of original grain shapes. It seems quite clear that these lunar materials are partly to completely recrystallized mineral grains and do not represent fragments of lunar anorthosite, pyroxenite, or dunite.

FIGURE 10. — Photomicrographs of Apollo 14 rocks. *A*, Photomicrograph of a clast of spherulitically recrystallized feldspar. 14301,16. *B*, Photomicrograph of olivine hornfels microclast with granoblastic-polygonal texture. 14066,5. *C*, Photomicrograph of olivine microclast, showing partial recrystallization of single kink-banded olivine grain. 14066,7. *D*, Photomicrograph of partly reacted olivine microclast surrounded by a corona of pyroxene and an opaque mineral. Note lightened halo in matrix around corona. Small "olivine" adjacent to right side of large one is completely replaced. 14308,3. *E*, Photomicrograph of a plagioclase porphyroclast in a poikiloblastically recrystallized D_2 metaclastic rock. Plagioclase porphyroclast has a narrow sodic reaction rim. 14063,8. *F*, Photomicrograph of red spinel microclasts with colorless feldspathic reaction rims. Largest spinel grain (lower center) has darkened borders next to the corona, while smaller grains are dark throughout. 14171,13. *G*, Photomicrograph of quartz microclast, crossed nicols, showing quartz core surrounded by an envelope of glass that in turn is surrounded by a corona of pyroxene. 14066,7. *H*, Photomicrograph of clast of partly fused graphic quartz-alkali feldspar intergrowth, crossed nicols. Fusion occurs along grain boundaries (wide black bands) in the interior of the clast. Quartz at the edge of the clast has reacted with the matrix to form a pyroxene corona. 14305,102. Bar scale 0.5 mm long.

MATRIX MATERIALS

Examination of surface photographs of boulders of breccia ejected from Cone crater (Hait, 1972) has shown the presence of some clasts that are larger than many of the returned samples. Since many of the clasts in the breccias are themselves fragments of breccia, the relative age of the "matrix" of any particular breccia sample is difficult to establish. The problem of distinguishing the youngest, or Fra Mauro, matrix is discussed in a later section; in the following discussion, "matrix materials" refers to the youngest binding agents of any particular sample.

It is apparent in hand sample and thin section that the clasts in the Apollo 14 fragmental rocks have a seriate distribution and that our division by grain size into clasts (>1.0 mm) and microclasts (0.1–1.0 mm) is arbitrary. Aside from a major increase in proportion of mineral microclasts in all rocks and of glass microclasts in those rocks that contain glass, the types and relative abundances of microclasts do not differ significantly from those of clasts. A comparison of the kinds of lithic clasts and lithic microclasts in the same rock (fig. 6) show that the proportions of rock types are much the same. Indeed, the grain sizes of the most abundant lithic clasts are such that they are commonly not disaggregated in the 0.1- to 1.0-mm-size fraction. One cannot readily account, therefore, for the origin of the large percentage of mineral fragments in the 0.1–1.0-mm size range. (See fig. 6.) A small proportion of these fragments were almost certainly derived by comminution of porphyroclasts in metaclastic rocks; for example, some plagioclase fragments are broken across sodic reaction rims that characterize these porphyroclasts. However, in most rocks, the proportion of plagioclase fragments is not high enough to suggest a porphyroclast source. Moreover, the comparative abundance of mineral microclasts is not matched by the generally low proportions of porphyroclasts, and the typical size of porphyroclasts is not larger than the mineral fragments. A more likely source for the

mineral fragments is the coarser grained gabbros with hypautomorphic granular texture. The mineral proportions in the clasts of gabbro are consistent with the mineral fragment distributions, although the relative paucity of gabbroic rocks among the lithic clasts is difficult to explain.

Rocks containing much clastic glass in the >0.1-mm-size fraction (F_1, F_2) also appear to be bound by glass that, if fragmental, is too small to resolve microscopically in thin sections.[3] Rocks lacking glass clasts (F_3, F_4) are bound by very finely crystalline apparently annealed material that is generally finer grained than most clasts of metaclastic rock. In some of these rocks, spherical and broken spherical fragments that presumably were formerly glass are now composed of fine crystalline material. Warner (1971, 1972) has subdivided the Apollo 14 breccias, using the relative abundance of glass clasts and of glass in the matrices as his principal criteria. He thus divided the rocks into six categories (from glassy "detrital" breccias to glass-free "annealed" breccias), which span our F_1–F_4 types.

MATRIX-CLAST REACTIONS

In a number of fragmental rocks, partial to complete reequilibration reactions have taken place between youngest matrices and some clasts and have clearly occurred subsequent to the formation of the breccia. In other rocks, similar reactions have been observed within the clasts but not within the youngest matrix, which suggests that these reactions are preconsolidation features.

Postconsolidation mineral reactions.—Mineral clasts and microclasts of olivine, plagioclase, spinel, and quartz commonly have reacted with the matrix containing them. Reaction products of olivine and matrix are orthopyroxene and ilmenite (fig. 10*D*). The apparent proportions of reaction products vary widely. The matrix appears in places to have been lightened in a faint halo around reacted grains (fig. 10*D*) to form a rim half as wide as the original diameter of the olivine. Irregular clasts of plagioclase commonly are surrounded by a narrow reaction rim of more sodic plagioclase (fig. 10*E*); in one example, reversed zoning was observed. Pale-pink to orange- or red-brown clasts of spinel(?) typically have reacted with the matrix to produce a compositional zoning (darkening) on the spinel and a corona of colorless, often radially fibrous material (feldspar) (Roedder and Weiblen, 1972; fig. 10*F*). Quartz has reacted with the matrix to form a corona of pyroxene; the pyroxene rim is typically separated from the quartz by a thin band of colorless glass (fig. 10*G*). In addition, both orthopyroxene and clinopyroxene appear to be compositionally zoned by reaction. Opaque minerals have also reacted, but these have not been closely examined.

The degree of reaction between minerals and matrix of the breccia containing them is very erratic, and grains showing well-developed reaction may occur side by side with those showing no reaction. However, there does appear to be a general sequence of reaction and also a correspondence between degree of recrystallization of the matrix (Warner, 1971, 1972) and degree of reaction. The earliest sign of reaction is the conversion of olivine to orthopyroxene + ilmenite. Interchange of components between the olivine and matrix is shown by light halos around such reaction rims. This reaction is observed in rocks in which no other minerals are visibly affected. The next reaction that occurs at a stage at which the pyroxene-ilmenite rims on olivine are still poorly developed is peripheral darkening of translucent spinel grains. Compositional zoning of plagioclase is commonly observed in rocks in which some olivine grains are completely reacted, and spinel grains may exhibit coronas of radially fibrous plagioclase. The olivine reaction is at best poorly developed in the glassy rocks; hence, the other, more advanced reactions probably occurred concomitantly with crystallization or recrystallization of the matrix of those rocks that now contain little or no glass. Careful examination of the phases involved may allow definition of facies of metamorphism. However, it should be emphasized that disequilibrium is the rule in these rocks and that meaningful temperature-pressure conditions of metamorphism will be most difficult to ascertain.

Table 7 summarizes the observed reaction phenomena. The two F_2 rocks contain fairly abundant glass clasts and microclasts. The remainder of the rocks exhibiting this reaction are classified as F_4; only one (14306) contains a minor amount of glass. All the rocks in which we have observed the reacted plagioclase and spinel are type F_4 and glass free.

Preconsolidation mineral reactions.—The same evidence of disequilibrium is found between porphyroclasts and their matrix in individual clasts as between mineral fragments and the youngest matrix in certain fragmental rocks: olivine has reacted to form ortho-

TABLE 7. — *Distribution of mineral reactions*

Sample No.	Rock type	Mineral reaction
14301	F_2	Olivine.
14307	F_2	Do.
14304	F_4	Olivine, spinel, plagioclase.
14306	F_4	Do.
14308–14311	F_4	Do.
14319	F_4	Do.
14321	F_4	Do.

[3]This type of glass differs conspicuously from "splash" glass that also cements some breccias, the largest of which is 14306. The "splash" glass contains very irregularly distributed fragmental material and is highly vesicular.

pyroxene and ilmenite, plagioclase has developed a sodic rim, and spinel has reacted to form a felsic(?) corona and complementary compositional zoning within the spinel. We have, in fact, noted these reactions in clasts in all of the rocks in which matrix-mineral clast reactions were noted above. In addition, we have observed reaction rims in clasts in several glassy fragmental rocks in which no young matrix reactions were seen. These rocks include members classified as types F_1, F_2, F_3, and F_4. We can only conclude that the reequilibration that affected these clasts took place prior to their incorporation into the Apollo 14 fragmental rocks.

PARTIAL FUSION

In several fragmental rocks (14270, 14303, 14305, 14306, 14315, 14318), quartz and quartz-alkali feldspar intergrowths were partly melted. Isolated quartz grains and those at the edges of quartz-feldspar clasts have colorless glass rinds that have reacted with the matrix to form characteristic pyroxene coronas. In the interiors of quartz-alkali feldspar clasts, partial fusion began along the grain boundaries of quartz and feldspar (fig. 10*H*). As in the mineral reactions described above, the effects of partial fusion are quite erratic, with extensively fused clasts occurring side by side with similar clasts showing no fusion. Partly melted clasts occur both as fragments isolated in the matrix of the rock and as clasts within larger fragmental clasts. In general, evidence concerning the time of melting, before or during formation of the breccia, is ambiguous. In one sample, however, melting clearly occurred after consolidation of the breccia: a melted part of a fragment of the metaclastic rock has intruded adjacent matrix (fig. 11*A*). Similarly, reaction between the matrix and partly melted quartz at the edges of some clasts also indicates fusion after formation of the breccia.

In some rocks, the glass resulting from partial fusion of quartz-feldspar intergrowths is the only glass remaining in the rock. (See also Dence and others, 1972.) In other rocks, material composed of fine-grained alkali-feldspar(?)-bladed quartz intergrowths suggests that melted clasts have devitrified. Devitrified quartz-feldspathic material is remarkably similar, both texturally and in mode of occurrence as both angular clasts and irregularly "intrusive" bodies, to Apollo 12 rock 12013 (Drake and others, 1970; James, 1971).

DEFORMATION OF MINERAL AND LITHIC CLASTS

All the varieties of mineral and lithic debris in the fragmental rocks described above show various degrees of deformation. Most plagioclase microclasts are mildly deformed by fracturing, and many show weak lattice distortion by undulose extinction; some are more severely deformed, as evidenced by mosaic texture and conversion to maskelynite. Many pyroxene microclasts are undeformed or weakly fractured, but some have well-developed shock-formed planar structures. Olivine microclasts are more commonly deformed, usually by development of broad kink bands.

The lithic fragments responded in the same ways to deformation. Some of them have textures ranging from those of weakly deformed cataclasites to severely shocked rocks in which maskelynite is well developed. Cataclastic rocks, composed of partly crushed, incompletely recrystallized material, are especially conspicuous among the small fraction of coarse-grained gabbroic clasts (fig. 11*B*). Apparently plagioclase is more susceptible to recrystallization in these rocks, and the mafic silicates remain as crushed aggregates. Isolated mineral clasts, especially of olivine and pyroxene, closely resembling the same minerals in these cataclasites, occur sparsely in the fragmental rocks. Marginal crush zones and partial mixing with debris of the host rock matrix (fig. 11*C*) indicate that some cataclasis occurred after isolation of the clast from its source rock. This texture is remarkably similar to marginal crush zones on clasts in the impact breccias of the Vredefort ring, South Africa (Wilshire, 1971).

Gradations from crushed rock that still retains its original textural identity to highly disaggregated debris in which fragments of neighboring minerals have been partly mixed are observed. Cataclastic deformation of an olivine-bearing rock of intermediate composition may have been the source of a small piece of soil breccia interpreted by Taylor and Marvin (1971) as fragmented dunite that was invaded by noritic matrix material.

Some gabbroic rocks (fig. 11*D*) are laced by irregular crush zones showing varying degrees of recrystallization, and some olivine clasts show moderate to extensive crushing. Most anorthosite clasts that are moderately crushed were polycrystalline aggregates whose original textures appear to have been metamorphic. Some partly crushed gabbros have igneous textures, others are too small to determine the original texture. Finer grained light-colored cataclastic rocks may represent cataclastically deformed cumulates or D_2 metaclastic rocks (table 4), and dark ones may have been derived from both basaltic rocks and D_4 metaclastic rocks (table 4). Severely shocked rocks in which maskelynite is well developed include intersertal basalts, D_2 metaclastic rocks, gabbros, and plagioclase cumulates.

COMPOUND CLASTS

Virtually every rock examined contains some compound clasts (fig. 11*E–G*), and in many, such clasts

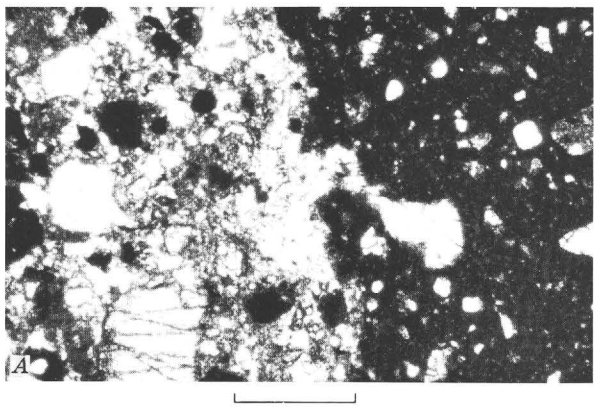
A

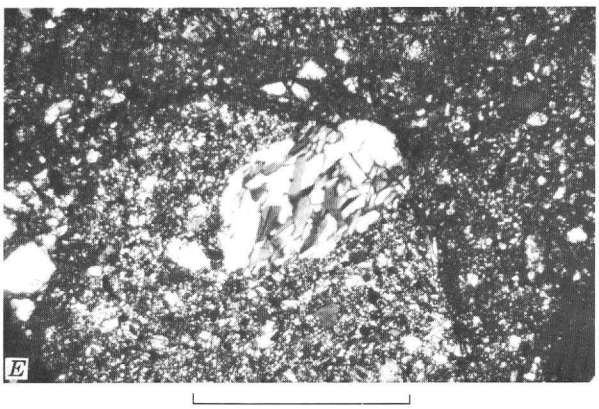
E

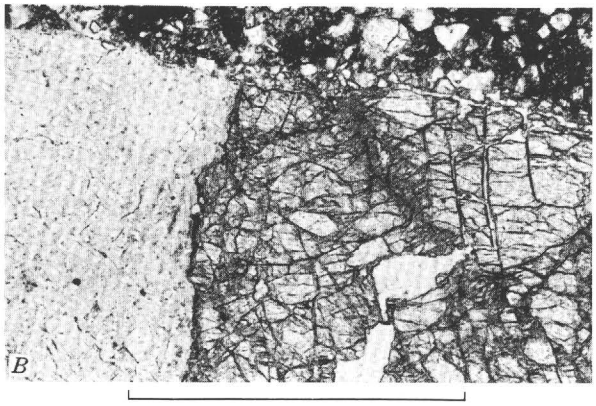
B

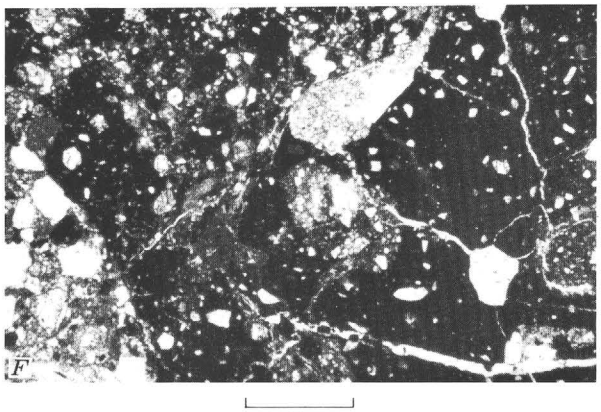
F

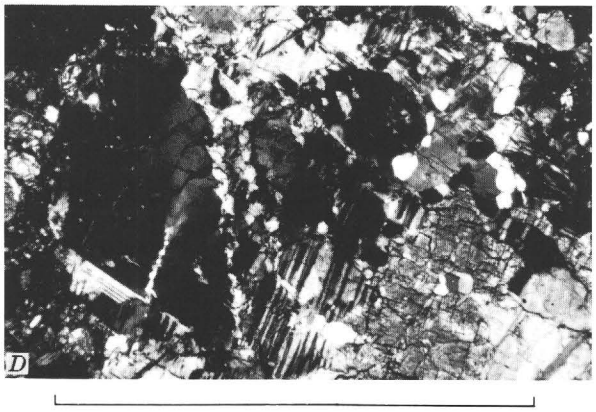
D

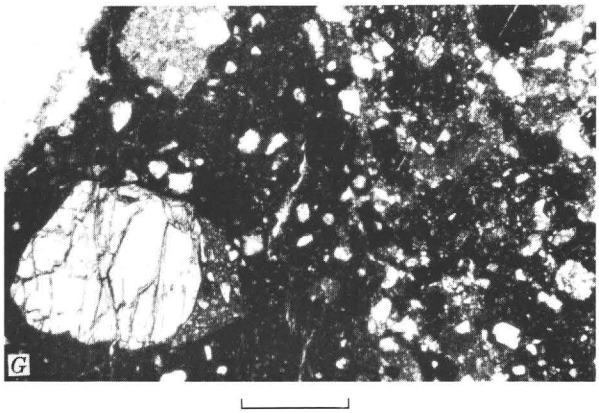
G


C

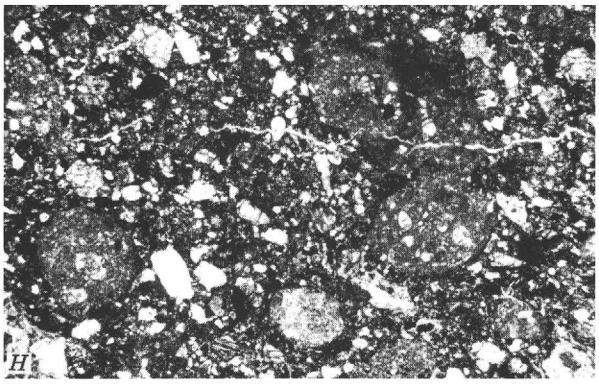
H

are abundant. Many of these are clearly fragments of breccias within which clast and matrix are readily identified. Others consist of two or more lithologies without a clear host-clast relation; usually, however, this can be ascertained by examination of several sections. In table 8 the common compound clasts are listed with the host lithology and clasts identified. The first column of table 8 gives the sample number and the main types of simple, noncomposite clasts observed. (See fig. 6 for the range and proportion of clast types in the entire sample.) For the most part, host-clast lithologies are present as simple clasts in the sample.

It is significant that only one of the compound clasts examined has an igneous host, the remainder being either light or dark metaclastic rocks. There is much greater variety among the included clasts than within their hosts; these clasts include not only an abundance of metamorphic rocks, but also cumulates, graphic quartz-alkali feldspar intergrowths, and intersertal, ophitic, and intergranular basalts. In contrast to simple clast populations, intergranular basalts are more abundant than intersertal and ophitic types. More rarely, a third generation of breccia is evidenced by clasts enclosed in second-stage clasts (table 8, column 3), and in one example (14308), a probable fourth generation was recognized (table 8, column 4). Four generations of breccias were also observed in sample 14321 by Duncan and others (1972).

TABLE 8. — *Clasts and matrix types in compound clasts*

Sample No.; main types of simple clasts	Host clast 1	Clasts in 1 2	Clasts in 2 3	Clasts in 3 4
14042—A_1, D_2	Glass	D_4, A_1		
14047—A_1, A_2, D_2	Glass	D_2, A_1		
14049—A_1, D_2	Glass	D_2		
14063—D_4	D_4	D_1, D_2		
14066—D_4	D_2	D_5, C_7, D_2, D_1		
	D_4	D_2		
14301—D_2	D_2	C_3, C_7, D_1, D_2, D_5		
	D_4	C_1, C_7, D_1		
14303—D_4	D_4	C_6, D_2		
14304—D_4	D_4	D_1, D_2, D_5		
14305—D_4	D_4	D_1, D_2		
14306—D_4	D_4	C_1, D_1, D_4	D_2, D_4	
14307—D_2	D_2	D_5, D_1		
	D_4	C_3, D_3		
	D_3	D_1, D_4		
14308—D_4	D_4, D_4	D_2	D_4	D_5
14312—D_4	D_4	D_4		
14313—A_1, D_4	C_5	D_2		
	D_4	D_4		
	D_2	D_4		
14314—D_4	D_4	D_2, D_4, D_5, C_7		
14315—D_2, D_4	D_4	A_2, C_2, D_4		

In one sample (14306), the clasts within host D_4 clasts were counted; although the proportions of these clasts are measurably different from those of the first generation of breccia, the essential properties of the F_4 class of rock 14306 are retained (compare positions for I3c and 14306 in fig. 12*A* and *B*). It is interesting and significant that older generations of clasts are of metaclastic rocks, clearly showing a history of multiple brecciation and metamorphism.

CLASSIFICATION OF THE ROCKS

Our classification of the Apollo 14 hand specimens is based primarily on coherence and on proportion of light and dark clasts and secondarily on the abundance of clasts and the proportion of glass (Jackson and Wilshire, 1972). The abundance of clasts (again arbitrarily limiting this term to fragments greater than 1 mm in diameter) is difficult to evaluate in thin sections, both because of the small sample size represented even by many sections and because of sectioning effects. Nevertheless, insofar as we could judge, the observations from hand specimens were supported by those from thin sections. We had difficulty in finding 1.0-mm fragments in rocks that we had classified as F_1 and F_3, but no difficulty in making statistically meaningful counts of clasts in types F_2 and F_4. (See fig. 6.) Considering the relative abundance of the different clast types (fig. 6), it is clear that the light and dark clasts serving as a basis for the hand-specimen classification are predominantly light and dark metaclastic rocks. In the following section, other less abundant lithic clast types are added to the light or

FIGURE 11. — Photomicrographs of Apollo 14 rocks. *A*, Photomicrograph of a completely melted quartz-alkali feldspar(?) clast in a dark metaclastic (D_4) clast. The glass was squeezed out of the clast and intruded into the adjacent matrix. 14306,65. *B*, Photomicrograph of cataclastically crushed "troctolite." Close view of crushed but not sheared olivine and plagioclase aggregate. 14083,8. *C*, Photomicrograph of crushed zone along edge of anorthosite clast. Top of photograph is normal dark matrix of the host rock; below that is a partly mixed zone (now recrystallized), followed downward in the photograph by unmixed crushed anorthosite, and at bottom by relict anorthosite, crossed nicols. 14306,3. *D*, Photomicrograph of gabbro clast laced by thin crush zones now partly recrystallized, crossed nicols. 14321,21. *E*, Photomicrograph of compound clasts. Clast of plagioclase hornfels with decussate texture in a finer grained D_2 metaclastic clast. 14306,60. Crossed polarized light. *F*, Photomicrograph of compound clast in coarse light-colored matrix (lower left corner of photograph). Clast is composed of several dark aphanitic fragments of metaclastic rock (D_4) in a fine-grained slightly lighter matrix. The largest clast (right side) has light-colored metaclastic (D_2) clasts within it. 14306,54. *G*, Photomicrograph of compound clast. Dark aphanitic (D_4) clast (left half of photograph) encloses two clasts of light metaclastic rock (D_2), the top one of which contains a large kink-banded olivine porphyroclast. 14306,4. *H*, Photomicrograph showing "pellet" texture characteristic of F_2 rocks. Round particles in field of view are metaclastic rocks, but well-rounded variolites, vitrophyres, and intersertal basalt fragments also are present in the rock. 14318,44. Bar scale 0.5 mm long.

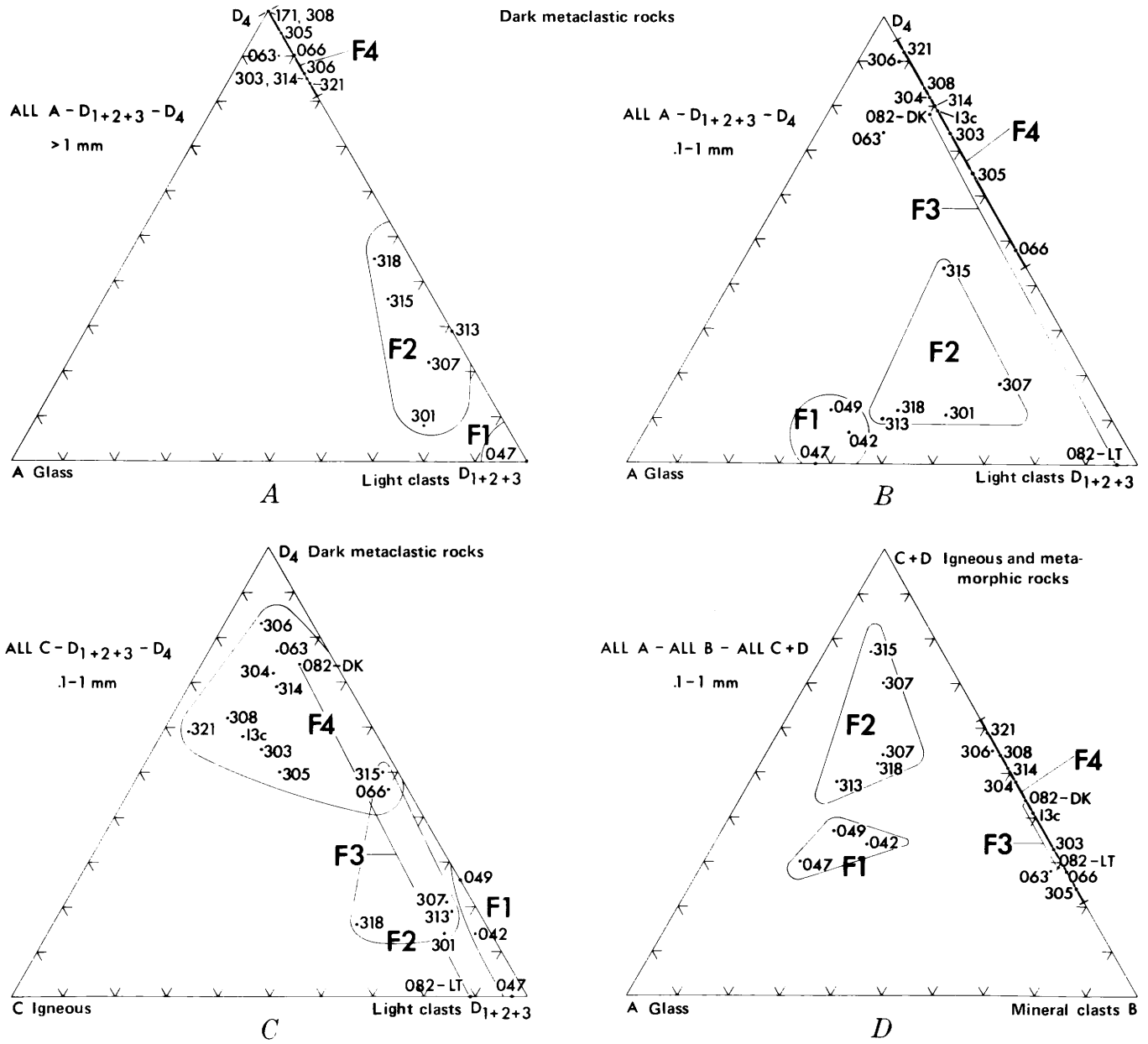

FIGURE 12. — Triangular plots of clasts and microclasts of glass, igneous, and metamorphic rocks. *A*, Triangular plot of glass (A), light-colored metamorphic rocks (D_1–D_3), and dark-colored metamorphic rocks (D_4), showing fields of rock groups F_1, F_2, and F_4. *B*, Triangular plot of microclasts, as in part *A* above. *C*, Triangular plot of clasts of igneous rocks (C), dark-colored metamorphic rocks (D_4), and light-colored metamorphic rocks (D_1–D_3), showing fields of rock groups F_1, F_2, F_3, and F_4. *D*, Triangular plot of clasts of igneous and metamorphic rocks (C and D), glass (A), and mineral grains (B), showing fields of rock groups F_1, F_2, F_3, and F_4.

dark metaclastic rock proportions where appropriate, but the same results would be obtained if they were ignored.

Coherence was impossible to measure in thin section, but the percentage of glass clasts was not. Figure 12*A* shows a triangular plot comparing the proportion of glass clasts to those of light-colored rocks (the total of D_1, D_2, and D_3 types) and dark-colored rocks (D_4) in thin sections available to us. A clear separation is found between F_1, F_2, and F_4 types in terms of light- and dark-clast ratios. It is also apparent that the F_2 rocks are more apt to contain glass than the F_4 types. Much better statistical reliability can be obtained from the microclast data. The same plot for fragments in the size range 0.1 to 1.0 mm is given in figure 12*B*. The same clear separation of light and dark clasts of F_2 and F_4 rocks is apparent. Furthermore, the proportion of D_4 clasts in F_1 rocks is, on the average, even

less than that of F_2, although some overlap is seen. The proportion of glass microclasts is also significantly different between groups — only two rocks classified as F_4 types contain glass microclasts, whereas all of the F_2 types contain significant amounts, and F_1 rocks contain more than 50 percent glass in this size range. Only two F_3 rocks were available for counting, and sample 14082 proved to be layered; the counts suggest that its darker layered component is like that of F_4 material, whereas its lighter component is unlike any of the other rocks. Sample 14063 has the same clast distributions as the F_4 group, but differs in having a white friable matrix.

A plot of microclasts of igneous rocks (all of group C in table 3) against dark (D_4) and light (D_1, D_2, and D_3) metamorphic rocks is given in figure 12*C*. The light and dark metamorphic rock separation is again apparent between F_4 and F_1–F_2 groups. The proportion of igneous rocks in the F_1 rocks is clearly very low, and there is an apparent tendency for F_2 rocks to contain fewer igneous rock clasts than F_4 rocks, although the areas overlap somewhat.

Finally, all lithic microclasts were plotted against glass and mineral fragments in figure 12*D*. While the clear separation of types F_1, F_2, and F_3 is largely due to glass content, it is apparent that type F_2 contains considerably higher proportions of lithic than mineral fragments in this size range. In contrast, the reverse is generally true for the other groups. F_4 rocks tend to have higher pyroxene-plagioclase ratios than F_1 and F_2 rocks.

With these features in mind, we can summarize the megascopic and microscopic characteristics of the four classification groups.

Rocks in the F_1 category are friable and contain few clasts larger than 1.0 mm. Where such clasts occur, they are very dominantly light colored. In the microclast size range, fragments consist of more than 40 percent glass with respect to mineral and lithic fragments. Mineral fragments are composed of 50–60 percent plagioclase, 35–50 percent pyroxene, and less than 10 percent olivine. Lithic fragments are strongly dominated by light-colored metamorphic rocks; igneous rocks make up less than 5 percent of the total lithic microclast population. Reactions between clasts or microclasts and matrix have not been observed, and multiple clasts are rare.

Rocks in the F_2 category are moderately coherent to coherent, contain abundant clasts, and have a striking pelletlike texture (fig. 11*H*). The clasts are dominantly light colored, but not so exclusively as those of F_1 rocks. In both clast and microclast size ranges, the fragments consist of more than 50 percent lithic fragments with respect to mineral and glass fragments. Glass fragments are everywhere present, however. Mineral fragments are principally plagioclase (60–90 percent), but olivine and pyroxene occur in a wide range of proportions (fig. 6). Lithic fragments are dominated by light-colored metamorphic rocks but contain 5–30 percent igneous rock fragments. Reactions between clasts or microclasts and matrix are present in at least two samples, but, in general, they are poorly developed or absent.

Only two rocks in the F_3 category were sectioned, and both have friable white crystalline matrices. One of these exhibited rather unusual banding. The dark bands exhibit F_4 properties in general (figs. 12*B–D*), but the rock is more friable. The light bands contain no D_4-type clasts and hence are unlike any of the other groups. The second rock resembles the dark bands in the first.

Rocks in the F_4 category are the most abundant in the collection. They are moderately coherent to tough and contain abundant clasts that are generally more angular than those in F_2 rocks. The clasts are dominantly dark colored, to the extent that there is no overlap in this respect with F_1 and F_2 rocks. In both the clast and microclast size ranges, glass is very scarce (figs. 12*A*, *B*); it has been observed only in two rocks in this category and then in minor amounts. Mineral fragments are relatively abundant with respect to lithic fragments and have approximately the same proportions as do those of F_2 rocks (fig. 7). Lithic fragments are dominantly dark metaclastic rocks, which make up 50 percent or more of the lithic clasts (fig. 12*C*). Igneous rocks show a wide range (4–20 percent) of relative lithic clast abundance. Reactions between clasts or microclasts and matrix are common and occur in at least five of the rocks we examined in thin section.

We emphasize that this classification is descriptive. Without intending to imply a genetic connotation, we note that the F_1 group of fragmental rocks corresponds to the "porous, unshocked microbreccias," and the F_3 and F_4 groups to the "thermally metamorphosed microbreccias" of Chao, Boreman, and Desborough (1971).

ROCK DISTRIBUTION

Figure 13 shows the field distribution of F_1–F_4 rocks (locations are from Sutton and others, 1971). Homogeneous crystalline rocks, believed to be clasts broken free from F_2 and F_4 fragmental rocks, are not shown on the map. It is at once apparent that the sample abundance is heavily weighted toward sites close to the lunar module. This would be even more conspicuous if samples smaller than 50 g were deleted. However, there is a regular pattern in the rock-type distribution:

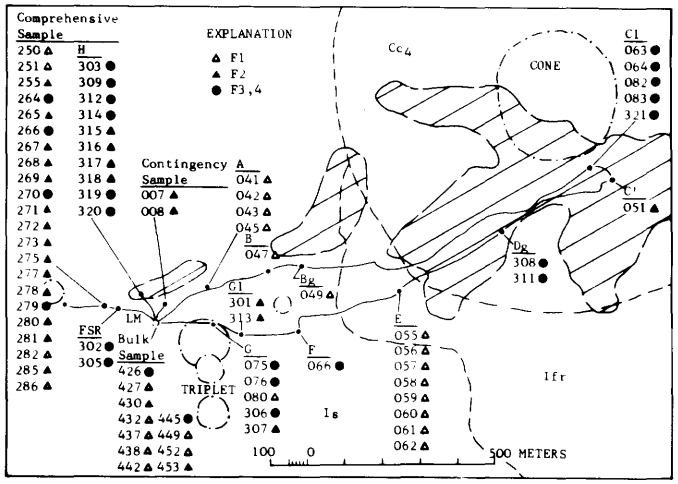

FIGURE 13. — Distribution of fragmental rock types at the Apollo 14 landing site.

1. All F_1 types were collected from the smooth terrain (fig. 2) outside the continuous ejecta blanket and blocky rays of Cone crater.
2. The great majority of F_2 rocks were collected from sites far removed from Cone crater (fig. 13), and some were almost certainly collected from the discontinuous outer parts of the Cone crater ejecta (Swann and Field Geology Team, 1971). F_4 type rocks also make up a sizable proportion of rocks collected from the outer part of Cone crater ejecta (fig. 13).
3. With the single exception of rock 14051, which was thoroughly dust covered when examined and may well be incorrectly classified, the samples collected from near the rim of Cone crater are F_3 and F_4 types. (See also Quaide, 1972.) That dark-clast-rich breccias are indeed the dominant variety of rock near Cone crater is further supported by the astronauts' descriptions and by the surface photographs of boulders on the flanks of Cone crater (Swann and Field Geology Team, 1971; Hait, 1972).

In terms of the general sequence of deposits in ejecta blankets (Shoemaker, 1960), the material collected from closest to the crater is presumed to represent the lowest units reached during crater excavation. At Cone crater, that material is fragmental rock with dominantly dark clasts (F_3 and F_4). Material collected from farther out on the ejecta blanket (F_2 and F_4) is presumed to represent material from higher levels in the precrater section. Whether the mixture of F_2 and F_4 types in ejecta at the outer, discontinuous part of the Cone crater rays (fig. 13) is due to a thin layer of F_2 or to complex intermingling of rocks by ejection through precrater fractures (Gault and others, 1968) cannot be ascertained.

Our interpretation, therefore, is that the lithologic units described above are stratified in the ridgelike terrain excavated by Cone crater. The surface of the stratigraphic pile away from the young ejecta blanket of Cone crater consists of soils and weakly lithified soil breccias (F_1). Light-clast-dominant coherent but glassy fragmental rocks (F_2) form the upper strata and most likely crop out in the upper walls of Cone crater. A still deeper unit of dark-clast-dominant coherent largely crystalline fragmental rocks (F_4) was penetrated by the Cone impact, and these rocks are concentrated near the rim. The unique "white rocks" (F_3) form layers in dark-clast-dominant fragmental rocks close to the rim of Cone crater and are presumed to represent the lowest parts of the section excavated by Cone crater (Sutton and others, 1972; Hait, 1972).

FRA MAURO FORMATION

Whether the stratigraphic units described in the preceding section represent unmodified Fra Mauro Formation, reworked or partly reworked Fra Mauro Formation, or more than one formation remains an open question. The pre-mission map of the Cone crater area (Eggleton and Offield, 1970) shows craters of Eratosthenian age as much as half a kilometer in diameter and a crater of Imbrian age approximately 1 km in diameter located in the immediate vicinity of the landing area. Shoemaker (1972) further contends that the Fra Mauro surface was in a steady state for craters as much as 1 km in diameter; if so, this suggests considerable reworking of the upper parts of the original Fra Mauro deposits. In the immediate vicinity of the landing site, known craters half a kilometer in diameter may be expected to have ejected materials over the future Cone crater site to depths of perhaps 5–15 m (H. J. Moore, oral commun., 1972). This is considerably less than the section ultimately sampled by the Cone event. If unrecognized larger impacts did indeed affect the Fra Mauro surface in the vicinity sampled, it is apparent that they did not modify the radial ridge pattern typical of the Fra Mauro surface. Hence, the bulk of the material ejected from Cone crater probably represents strata deposited before the oldest craters in the immediate area were formed.

The uppermost units (F_1–F_2) at the Apollo 14 landing site are lithologically distinct from underlying units and cannot be the result of reworking of lower units, despite suggestions to the contrary (Quaide, 1972; Dence and others, 1972). Hence, they must represent either the uppermost surviving units of the Fra Mauro Formation or younger, post-Fra Mauro rocks. The only tangible evidence we have bearing on this question is apparent gradational thermal behavior between F_2 and F_4 rocks: metamorphic reactions be-

tween mineral clasts and matrix are much better developed in F_4 rocks, but olivine has reacted locally with the glassy matrix of F_2 breccias. This suggests that F_2, F_3, and F_4 breccias represent a single cooling unit of the original Fra Mauro Formation.

The viability of our conclusions is dependent on the correct recognition of the Fra Mauro matrix proper. The presence of breccia clasts in boulders ejected from Cone crater that are bigger than many of the returned samples does not allow an *a priori* identification of the youngest matrix in any particular sample as Fra Mauro. However, the packing density of identifiable large clasts is quite low (Hait, 1972), and the probability of sampling the youngest breccia matrix in the boulders appears to be high. If the boulders around Cone crater are themselves clasts in the Fra Mauro matrix, the minimum clast size would have to be larger than several meters. "Turtle Rock" (Sutton and others, 1971), a 2-m-wide boulder in north boulder field, appears to have the same clast population as the two samples (14321, 14319) taken from the top of the boulder. Still larger boulders photographed near Cone crater show no signs of huge clast boundaries within them, and we find it difficult to believe that every block in the field is indeed a clast. Lacking tangible evidence to the contrary, we therefore presume that the youngest matrices of most breccia samples are the Fra Mauro proper and not matrices of older breccias.

If we accept the F_2, F_3, and F_4 rocks as samples of the Fra Mauro Formation and the idea that these rocks represent a single cooling unit, then local temperatures on the order of 1,000°C are required. (See also Quaide, 1972; Dence and others, 1972.) Terrestrial examples suggest that temperatures of this magnitude are restricted to areas relatively closer to the locus of impact. In the Ries basin (Germany), the best-known large terrestrial impact crater that retains its ejecta deposits, the high-temperature ejecta (suevite) extends out only about half a crater diameter (Pohl and Angenheister, 1969; Dennis, 1971), whereas lower temperature breccia deposits (Bunte Breccia) underlie the suevite and extend nearly a crater diameter from the crater rim (Dennis, 1971). However, these deposits have been subjected to lengthy erosion, and the suevite, being in the most easily eroded position, may originally have covered a much larger area. The view that the Apollo 14 high-temperature rocks are derived from earlier basin-forming events rather than from the Imbrium impact (Dence and others, 1972) does not solve the problem because the source area of the Fra Mauro rocks was just as distant from earlier major basins, such as Serenitatis or the south Imbrium basin (Wilhelms and McCauley, 1971), as the Apollo 14 site is from the Imbrium basin. We must conclude, therefore, that the magnitude of major lunar basin-forming events is such that small terrestrial craters do not provide adequate models for temperature distribution in the ejecta deposits.

CONCLUSIONS

The site descriptions at the Apollo 14 landing area and the nature of the rocks returned by the crew strongly support Gilbert's (1893) conclusion that the area is covered by ejecta from the Imbrium basin. We can apply petrologic observations to a more detailed interpretation of the nature and stratigraphy of the Fra Mauro Formation by attempting to reconstruct an inverted stratigraphic section in the Cone crater ejecta. And, on the basis of the clasts in what we believe to be Fra Mauro rocks, we can say something about the terrane that existed in the Imbrium area prior to the enormous impact that produced that basin.

FRA MAURO FORMATION

The distribution of rocks collected in the Apollo 14 landing area suggests that the Fra Mauro Formation is stratified. The deepest unit sampled is composed of fragmental rocks rich in dark clasts with interlayered white fragmental rocks (F_4 and F_3), the next overlying layer is composed of well-indurated fragmental rocks (F_2) rich in light-colored clasts, and the uppermost unit is unconsolidated to weakly lithified (F_1) regolith.

F_1 type fragmental rocks, characterized by an abundance of glass, weak lithification, and scarcity of clasts bigger than 1 mm, were collected from areas not covered by Cone crater ejecta, and in most respects they closely resemble the unconsolidated soils of the area (Carr and Meyer, 1972; Quaide, 1972). They appear to represent poorly lithified regolith that formed either by disaggregation and weak re-lithification of F_2 material or from an originally unconsolidated layer of fragmental material overlying the F_2 material. Comparison of the clast populations of F_1 and F_2 shows that F_1 has more clastic glass, much more pyroxene in the microclast size range, and fewer clasts of igneous rock than F_2. It is possible that all of these are effects of "gardening" of F_2 material by small impacts, which would tend to produce glass and break down the coarser grained clasts more rapidly than the fine-grained clasts. However, it remains possible that the regolith and F_1 rocks are derived from a surficial layer overlying F_2 material that was originally of a different composition.

In our opinion, F_2 rocks represent the upper, consolidated part of the Fra Mauro Formation and are probably exposed in the upper walls of Cone crater. Glass-filled fractures cross clasts and matrices alike in both F_2 and F_4 rocks and are presumably a consequence of the Cone impact, indicating that both rock

types were consolidated at the time of that event. The F_2 rocks contain some clastic glass, some of which was soft during consolidation of the rocks, and are partly bound by glass. Moreover, a few of these rocks show the earliest signs of postconsolidation metamorphic reaction between mineral clasts and the matrix. The simplest explanation of these features is that part of the ejecta was hot when deposited and that insulation and compaction by upper units allowed induration and metamorphism of lower units. The preservation of glass and very limited metamorphic reaction suggest that all these rocks were near the original top of the Fra Mauro ejecta blanket.

Comparison of the clast populations of F_2 and F_4 rocks, as well as their general textures, shows that these are distinctive rocks and lack intermediate types; this is especially evident in the relative abundance of light- and dark-colored metaclastic rocks. Hence, we infer that the contact between the F_2 and F_4 units in the Fra Mauro Formation is sharp. However, since neither glass nor metamorphic reactions are unique to F_2 or F_4, it seems likely that the thermal metamorphic effects are gradational across the contact. In this respect, the deposits are analogous to cooling units of welded tuff deposits.

F_3 and F_4 rocks represent the lower consolidated part of the Fra Mauro Formation sampled. These rocks are largely crystalline, and the original glass clasts and glassy matrix material have largely been annealed and devitrified. Postconsolidation metamorphic reactions are likewise considerably better developed than in F_2 rocks. This feature and the distribution of rocks around Cone Crater suggest a deeper source for F_4 rocks in which the thermal blanketing effect of overlying material allowed slower cooling and partial reequilibration of an assortment of material thrown together by impact. Local temperatures were high enough (about 1,000°C) to reset partially or completely certain radiogenic systems used to date the Apollo 14 rocks (Silver, 1972; Papanastassiou and Wasserburg, 1971; Turner and others, 1971; Compston and others, 1971), but the very erratic distribution of metamorphic reactions and partial fusion effects indicates uneven heating of debris in the blanket.

PRE-IMBRIUM TERRANE

The stratigraphic sequence inferred for samples collected from the Cone crater ejecta is based on interpretations gleaned from small terrestrial craters. Studies of these craters have shown that, in a general way, the stratigraphy of the target is inverted and that younger beds are exposed farther from the source in the ejecta blankets. Application of these general rules to the Imbrium basin is perhaps an unwarranted extrapolation, and we cannot be fully confident that ejected materials from such large basins will behave in the same way. However, it is noteworthy that the samples collected 550 km from the rim of the Imbrium basin, and only 150 km from the mapped edge of the ejecta deposit, are of a character suggesting a relatively shallow origin.

Glassy materials in the F_2 rocks were presumably produced during the Imbrium event and give little information on the lithologic character of the source material. The mineral microclast population, however, offers more potential. We have pointed out before that these clasts are too large and too numerous to have been supplied by disaggregation of the most abundant (fine-grained metaclastic rocks) clasts in the breccias. Early results from Apollo 15 (Wilshire and others, 1972) show that coarser rocks of appropriate composition were present in the Imbrium target area and that these may have supplied the mineral debris if comminution was nearly complete.

The lithic clasts in the Apollo 14 rocks are of a great variety, indicating a very complex target area of the Imbrium impact. Igneous clasts include fresh basalts of several varieties that are in general richer in feldspar than basalts from the mare regions and rocks with cumulus and hypautomorphic textures that suggest igneous crystallization and differentiation at depth. Metamorphic clasts, the dominant clast type in Apollo 14 rocks, are of both fine-grained dark-colored types and coarser light-colored types. All of them appear to have formed by impact fragmentation and thermal metamorphism, clasts of each type containing relicts of the fragmentation and incomplete reequilibration of materials during thermal metamorphism.

Both the igneous and metamorphic rock types are themselves clasts in the common compound breccia clasts. In the record revealed by small thin sections, as many as four fragmentation events have been recognized, each apparently followed by thermal metamorphism. These relations show that impact fragmentation and subsequent thermal metamorphism happened many times and that materials similar to the Fra Mauro Formation were themselves disrupted by the Imbrium event. It seems likely that the Serenitatis blanket, which must certainly have covered most of the Imbrium basin area (fig. 14), provided one generation of these materials.

Hence, the pre-Imbrium terrane, presumed to have existed prior to about 3.9 to 4.2 billion years ago (Silver, 1971, 1972; Wasserburg and others, 1971) was already exceedingly complex. Multiple ejecta blankets from very large impacts had been laid down and metamorphosed. Basalts had been erupted and incorporated in the ejecta blankets. Very likely, some flows

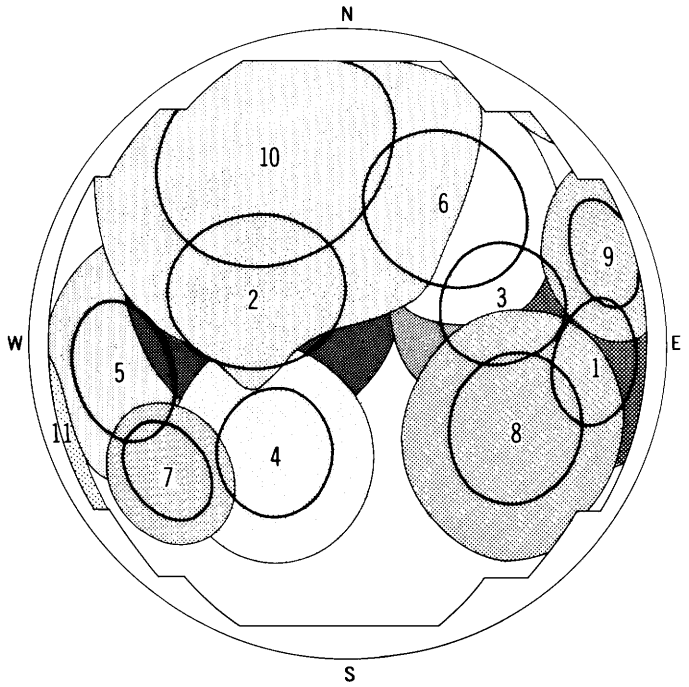

FIGURE 14. — Map showing main outer mountain rings of major lunar basins, their relative ages, and the extent of their continuous ejecta blankets (based on a Mare Orientale model for basins older than Imbrium). Drawn by D. E. Wilhelms, U.S. Geological Survey. 1, Fecunditatis. 2, "South Imbrium." 3, Tranquillitatis. 4, Nubium. 5, Procellarum. 6, Serenitatis. 7, Humorum. 8, Nectaris. 9, Crisium. 10, Imbrium. 11, Orientale.

were extruded in the Imbrium area itself, intercalated with these ejecta blankets. At depth, either in the Imbrium area or in still older basins, igneous intrusion, crystallization, and differentiation had occurred.

Processes operative prior to 3.9 to 4.2 billion years ago, so far as we can determine, were not unlike those operative later, and the Moon probably appeared then about the same as it does now. Hence, the existence of a primordial crust of "anorthosite" (Wood and others, 1970a, b) or "fused shell" (Smith and others, 1970) is not established. Rather, we see in the Fra Mauro clasts a long history of impact and ejection that probably records half a billion years of planetary accretion, of which the Imbrium impact was one of the last large events on the Moon.

REFERENCES CITED

Ave'Lallemant, H. G., and Carter, N. L., 1972, Deformation of silicates in some Fra Mauro breccias, *in* Third Lunar Sci. Conf., Houston, Texas, January 1972: Lunar Sci. Inst. Contr. 88, p. 33–34.

Carr, M. H., and Meyer, C. E., 1972, Petrologic and chemical characterization of soils from the Apollo 14 landing site, *in* Third Lunar Sci. Conf., Houston, Texas, January 1972: Lunar Sci. Inst. Contr. 88, p. 117–118.

Chao, E. C. T., Boreman, J. A., and Desborough, G. A., 1971, The petrology of unshocked and shocked Apollo 11 and Apollo 12 microbreccias, *in* Second Lunar Sci. Conf., Houston, Texas, 1971, Proc.: Geochim. et Cosmochim. Acta, Supp. 2, v. 1, p. 797–816.

Chao, E. C. T., Minkin, J. A., and Boreman, J. A., 1972, Apollo 14 glasses of impact origin, *in* Third Lunar Sci. Conf., Houston, Texas, January 1972: Lunar Sci. Inst. Contr. 88, p. 131–132.

Compston, W., Vernon, M. J., Berry, H., and Rudowski, R., 1971, The age of the Fra Mauro Formation — A radiometric older limit: Earth and Planetary Sci. Letters, v. 12, p. 55–58.

Dence, M. R., Plant, A. G., and Traill, R. J., 1972, Impact-generated shock and thermal metamorphism in Fra Mauro lunar samples, *in* Third Lunar Sci. Conf., Houston, Texas, January 1972: Lunar Sci. Inst. Contr. 88, p. 174–176.

Dennis, J. G., 1971, Ries structure, southern Germany, a review: Jour. Geophys. Research, v. 76, p. 5394–5406.

Drake, M. S., McCallum, I. S., McKay, G. A., and Weill, P. F., 1970, Mineralogy and petrology of Apollo 12 sample 12013 — A progress report: Earth and Planetary Sci. Letters, v. 9, p. 124–126.

Duncan, A. R., Lindstrom, N. N., Lindstrom, D. J., McKay, S., Woodbury, J. A., Goles, G. G., and Fruchter, J. S., 1972, Comments on the genesis of breccia 14321, *in* Third Lunar Sci. Conf., Houston, Texas, January 1972: Lunar Sci. Inst. Contr. 88, p. 192–194.

Eggleton, R. E., 1963, Thickness of the Apennine Series in the Lansberg region of the Moon, *in* Astrogeol. Studies Ann. Prog. Rept., August 1961–August 1962: U.S. Geol. Survey open-file report, p. 19–31.

Eggleton, R. E., and Offield, T. W., 1970, Geologic map of part of the Fra Mauro region of the Moon — Apollo 13: U.S. Geol. Survey Misc. Geol. Inv. Map I–708.

Fredriksson, K., Nelen, J., Noonan, A., and Kraut, F., 1972, Apollo 14 — Glasses, breccias, chondrules, *in* Third Lunar Sci. Conf., Houston, Texas, January 1972: Lunar Sci. Inst. Contr. 88, p. 280–282.

Gault, D. E., Quaide, W. L., and Oberbeck, V. R., 1968, Impact cratering mechanics and structures, *in* French, B. M., and Short, N. M., eds., Shock metamorphism of natural materials: Baltimore, Md., Mono Book Corp., p. 87–99.

Gilbert, G. K., 1893, The Moon's face — A study of the origin of its features: Philos. Soc. Washington Bull., v. 12, p. 241–292.

Hait, M. H., 1972, The white rock group and other boulders of the Apollo site — A partial record of the Fra Mauro history, *in* Third Lunar Sci. Conf., Houston, Texas, January 1972: Lunar Sci. Inst. Contr. 88, p. 353.

Jackson, E. D., and Wilshire, H. G., 1972, Classification of the samples returned from the Apollo 14 landing site, *in* Third Lunar Sci. Conf., Houston, Texas, January 1972: Lunar Sci. Inst. Contr. 88, p. 418–420.

Jakeš, Petr, and Reid, A. M., 1971, Petrology of the Fra Mauro Formation [abs.]: Geol. Soc. America Abs. with Programs, v. 3, p. 611.

James, O. B., 1971, Origin of lunar microbreccia 12013 [abs.]: EOS (Am. Geophys. Union Trans.), v. 52, no. 4, p. 272.

James, O. B., and Jackson, E. D., 1970, Petrology of the Apollo 11 ilmenite basalts: Jour. Geophys. Research, v. 75, p. 5793–5824.

King, E. A., Jr., Butler, J. C., and Carman, M. F., 1971, Apollo 14 sample results — Chondrule-like bodies, grain size analyses, and estimation of lunar surface ages [abs.]: Geol. Soc. America Abs. with Programs, v. 3, p. 623.

———1972, Chondrules in Apollo 14 breccias and estimation of lunar surface exposure ages from grain size analysis, *in* Third Lunar Sci. Conf., Houston, Texas, January 1972: Lunar Sci. Inst. Contr. 88, p. 449–451.

Lunar Sample Preliminary Examination Team, 1971, Preliminary examination of lunar samples from Apollo 14: Science, v. 173, p. 681–693.

McKay, D. S., Clanton, U. S., Heiken, G. H., Morrison, D. A., Taylor, R. M., and Ladle, G., 1972, Characterization of Apollo 14 soils, *in* Third Lunar Sci. Conf., Houston, Texas, January 1972: Lunar Sci. Inst. Contr. 88, p. 529–531.

Melson, W. G., Mason, B., Nelen, J., and Jacobson, S., 1972, Apollo 14 basaltic rocks, *in* Third Lunar Sci. Conf., Houston, Texas, January 1972: Lunar Sci. Inst. Contr. 88, p. 535–536.

Papanastassiou, D. A., and Wasserburg, G. J., 1971, Rb-Sr ages of igneous rocks from the Apollo 14 mission and the age of the Fra Mauro Formation: Earth and Planetary Sci. Letters, v. 12, p. 36–48.

Papike, J. J., and Bence, A. E., 1971, Apollo 14 pyroxenes: Subsolidus relations and implied thermal histories [abs.]: Geol. Soc. America Abs. with Programs, v. 3, p. 666.

Pohl, Jean, and Angenheister, Gustav, 1969, Anomalien des Erdmagnetfeldes und Magnetisierung der Gesteine im Nördlinger Ries, *in* Das Ries — Geologie, Geophysik, und Genese eines Kraters: Geol. Bavarica, no. 61, p. 327–336.

Quaide, W. L., 1972, Mineralogy and origin of Fra Mauro fines and breccias, *in* Third Lunar Sci. Conf., Houston, Texas, January 1972: Lunar Sci. Inst. Contr. 88, p. 627–629.

Ridley, W. I., Williams, R. J., Takeda, H., Brown, R. W., and Brett, R., 1971, Petrology of Fra Mauro basalt 14310 [abs.]: Geol. Soc. America Abs. with Programs, v. 3, p. 682.

Roedder, E., and Weiblen, P. W., 1972, Petrographic and petrologic features of Apollo 14 and 15 and Luna 16 samples, *in* Third Lunar Sci. Conf., Houston, Texas, January 1972: Lunar Sci. Inst. Contr. 88, p. 657–659.

Shoemaker, E. M., 1960, Penetration mechanics of high velocity meteorites, illustrated by Meteor Crater, Arizona: Internat. Geol. Cong., 21st, Copenhagen, 1960, Rept., pt. 18, p. 418–434.

———1972, Cratering history and early evolution of the Moon, *in* Third Lunar Sci. Conf., Houston, Texas, January 1972: Lunar Sci. Inst. Contr. 88, p. 669–698.

Silver, L. T., 1971, U-Th-Pb isotope relations in some Apollo 14 (and 15?) materials [abs.]: Geol. Soc. America Abs. with Programs, v. 3, p. 706.

———1972, Lead volatilization and volatile transfer processes on Moon, *in* Third Lunar Sci. Conf., Houston, Texas, January 1972: Lunar Sci. Inst. Contr. 88, p. 701–703.

Smith, J. V., Anderson, A. T., Newton, R. C., Olsen, E. J., and Wyllie, P. J., 1970, Petrologic history of the moon inferred from petrography, mineralogy, and petrogenesis of Apollo 11 rocks, *in* Apollo 11 Lunar Sci. Conf., Houston, Texas, 1970, Proc.: Geochim. et Cosmochim. Acta, Supp. 1, v. 1, p. 897–925.

Spry, A., 1969, Metamorphic textures: New York, Pergamon Press, 350 p.

Sutton, R. L., Batson, R. M., Larson, K. B., Schafer, J. P., Eggleton, R. E., and Swann, G. A., 1971, Documentation of the Apollo 14 samples: U.S. Geol. Survey open-file report, 37 p.

Sutton, R. L., Hait, M. H., and Swann, G. A., 1972, Geology of the Apollo 14 landing site, *in* Third Lunar Sci. Conf., Houston, Texas, January 1972: Lunar Sci. Inst. Contr. 88, p. 732–734.

Swann, G. A., and Field Geology Team, 1971, Preliminary geologic investigations of the Apollo 14 landing site, *in* Apollo 14 Prelim. Sci. Rept.: Natl. Aeronautics and Space Adm. Spec. Pub. SP–272, p. 39–85.

Swann, G. A., Trask, N. J., Hait, M. H., and Sutton, R. L., 1971, Geologic setting of the Apollo 14 samples: Science, v. 173, no. 3998, p. 716–719.

Taylor, G. J., and Marvin, U. B., 1971, A dunite-norite lunar microbreccia: Meteoritics, v. 6, p. 173–180.

Turner, Grenville, Huneke, J. C., Podosek, F. A., and Wasserburg, G. J., 1971, ^{40}Ar–^{39}Ar ages and cosmic ray exposure ages of Apollo 14 samples: Earth and Planetary Sci. Letters, v. 12, p. 19–35.

Warner, J. L., 1971, Progressive metamorphism of Apollo 14 breccias [abs.]: Geol. Soc. America Abs. with Programs, v. 3, p. 744.

———1972, Apollo 14 breccias — Metamorphic origin and classification, *in* Third Lunar Sci. Conf., Houston, Texas, January 1972: Lunar Sci. Inst. Contr. 88, p. 782–784.

Wasserburg, G. J., Huneke, J. C., Papanastassiou, D. C., Podosek, F. A., Tera, F., and Turner, G., 1971, Lunar chronology and evolution [abs.]: Geol. Soc. America Abs. with Programs, v. 3, p. 745.

Wilhelms, D. E., 1970, Summary of lunar stratigraphy — Telescopic observations: U.S. Geol. Survey Prof. Paper 599–F, p. F1–F47.

Wilhelms, D. E., and McCauley, J. F., 1971, Geologic map of the near side of the Moon: U.S. Geol. Survey Misc. Geol. Inv. Map I–703.

Wilshire, H. G., 1971, Pseudotachylite from the Vredefort ring, South Africa: Jour. Geology, v. 79, p. 195–206.

Wilshire, H. G., and Jackson, E. D., 1972, Petrology of the Fra Mauro Formation at the Apollo 14 landing site, *in* Third Lunar Sci. Conf., Houston, Texas, January 1972: Lunar Sci. Inst. Contr. 88, p. 803–805.

Wilshire, H. G., Schaber, G. G., Silver, L. T., Phinney, W. C., and Jackson, E. D., 1972, Geologic setting and petrology of Apollo 15 anorthosite (15415): Geol. Soc. America Bull., v. 83, p. 1083–1092.

Wilson, A. F., 1969, Some structural, geochemical, and economic aspects of the metamorphosed East Fraser gabbro and associated pyroxene granulites of the Fraser Range, Western Australia: Indian Mineralogist, v. 10, p. 46–66.

Wood, J. A., Dickey, J. S., Jr., Marvin, U. B., and Powell, B. N., 1970a, Lunar anorthosites and a geophysical model of the Moon, *in* Apollo 11 Lunar Sci. Conf., Houston, Texas, 1970, Proc.: Geochim. et Cosmochim. Acta, Supp. 1, v. 1, p. 965–988.

———1970b, Lunar anorthosites: Science, v. 167, p. 602–604.

☆GPO 781-165